General Stress-Strain Relationship for Concrete at Elevated Temperatures

M.A. Youssef*, M. Moftah

The University of Western Ontario, Department of Civil and Environmental Engineering, London, ON N6A 5B9, Canada

Abstract

A general stress-strain relationship for concrete when subjected to fire is needed as it allows designing concrete structures to specific fire-performance criteria and improves the understanding of the behaviour of these structures during fire events. Existing relationships are developed based on fire tests of unconfined concrete specimens. They provide significantly different predictions because of uniqueness of each relationship and the existence of numerous formulations for calculating the governing parameters. In this paper, available formulations for estimating the parameters affecting the behaviour of unconfined and confined concrete are presented. These parameters are concrete compressive strength, concrete tensile strength, concrete compressive strain at peak stress, initial modulus of elasticity of concrete, transient creep strain, thermal strain, and yield stress and bond strength of reinforcing bars. Recommendations for choosing specific formulations are made based on accuracy, generality, and simplicity. Suitable compressive and tensile stress-strain relationships at elevated temperature that utilize the recommended formulations are proposed based on well-established relationships for confined concrete at ambient temperature. The proposed relationships are compared to existing ones and available experimental data. They can capture changes in the mechanical properties of concrete resulting from temperature and confinement and are found to be superior to existing relationships. However, additional tests are needed to further validate and improve the proposed relationships.

Keywords: Concrete; stress-strain relationship, temperature; fire; transient creep; initial stress; thermal Strain; yield strength, tensile strength, compressive strength.

* Corresponding author. Tel.: +1 519 661-2111 Ext. 88661; Fax: +1 519 661-3779.
E-mail address: youssef@uwo.ca

1. Introduction

Engineers generally satisfy fire safety requirements by choosing floor and wall assemblies that satisfy specific fire ratings. Such a method does not require any temperature-dependent calculations. However, new codes are moving towards performance-based design and temperature-dependent calculations are expected to be required to satisfy certain performance criteria. A general stress-strain relationship for concrete when subjected to high temperature is thus needed. Such a relationship will also be beneficial to researchers interested in modelling the behaviour of concrete structures when subjected to fire.

Numerous models were developed during the last century to represent the compressive and tensile stress-strain behaviour of unconfined and confined concrete structures at ambient temperature. Elevated temperatures occurring during fire events were found to change the characteristics of the stress-strain relationships for unconfined concrete. A review of mechanical properties of concrete at elevated temperature is given by Phan and Carino [1]. Effects of elevated temperatures include decreasing concrete strength, f_c', [2-7] and increasing the absolute value of the strain corresponding to it (ε_o) [8-16]. Hertz [3], Lie [4], and Purkiss [7] reported that preloading concrete with a compressive stress f_{ci} reduces the effect of elevated temperatures on f_c' and ε_o. f_{ci} was also found to result in additional strains that were termed transient creep strains (ε_{tr}) [17-19]. The magnitude of these strains is a function of the heating rate, the concrete mix, and the preloading stress level. The effect of elevated temperature on the stress-strain relationship of confined concrete is not fully understood. Confinement is expected to be affected by the deterioration of the bond between the reinforcing bars and the surrounding concrete [5, 7, 8, 10] and the reduction in the yield stress of transverse reinforcing bars during fire [4, 6, 7]. Following a fire event, residual properties of concrete are of importance as they define the best rehabilitation strategy. Their values are different from those during fire [1,20].

In this paper, a review of existing models for concrete structures at normal and elevated temperatures is given. This includes effect of elevated temperatures on concrete compressive and tensile strengths, concrete compressive strain at peak stress, transient creep strain, yield strength of reinforcing bars, and bond strength of reinforcing bars. General stress-strain relationships are

proposed and examined using available experimental results. The paper also identifies tests that should be carried out to validate and improve the proposed models.

2. Compressive Stress-Strain Relationship for Concrete at Normal Temperature

The behaviour of concrete under compression is greatly affected by the degree of confinement provided by the transverse reinforcement. For unconfined concrete, a widely used approximation for the stress-strain relationship before maximum stress is a second-degree parabola. ε_o can be taken as 0.002 or $\frac{2 \cdot f_c'}{E_{ci}}$ [21], where E_{ci} is its initial modulus of elasticity. Mander et al. [22] recommended estimating E_{ci} as $5000.\sqrt{f_c'}$ MPa. The post peak behaviour can be estimated either by extending the equation of the second-degree parabola [23] or by using a linear decaying branch with a slope of $\frac{-0.15 \cdot f_c'}{0.0038 - \varepsilon_o}$ [21]. The length of the decaying branch is strongly affected by the conditions of the test. A number of values for the maximum strain (ε_{cu}) can be found in the literature. Those include 0.003 [24], 0.0035 [25], and 0.0038 [21]. Neville [26] proposed using equation 1 to take into account the reduction in ε_{cu} that was noted for higher strength concretes.

$$\varepsilon_{cu}(\text{unconfined concrete}) = 4.942 \times 10^{-3} - 6.995 \times 10^{-5} \cdot f_c' + 3.993 \times 10^{-7} \cdot f_c'^{\,2} \quad (1)$$

To account for effect of creep on the stress-strain relationship, It was suggested by Collins and Mitchell [27] to shift the strain at the maximum stress to be equal $\varepsilon_o + \varepsilon_{cr}$, where ε_{cr} is the creep strain at maximum stress.

Regarding confined concrete, a number of models exist in the literature [22, 28-31]. Two of the widely used models will be briefly described in the following paragraphs.

The model of Kent and Park [28] accounts for improvement in ductility due to confinement provided by rectangle hoops. The model was later extended by Scott et al. [29] to account for the improvement in strength. In this model, the monotonic concrete stress-strain relationship in compression, shown in Fig. 1, is described by equations 2a to 2f. The equations were modified to include the effect of creep in a similar approach to that suggested by Collins and Mitchell [27].

Before reaching the maximum stress ($\varepsilon_c \leq \varepsilon_{oc} + \varepsilon_{cr}$), the improvements in strength and ductility are accounted for by a confinement factor, K_h.

$$f_c = K_h f_c' \left[2.0 \left(\frac{\varepsilon_c}{\varepsilon_{oc} + \varepsilon_{cr}} \right) - \left(\frac{\varepsilon_c}{\varepsilon_{oc} + \varepsilon_{cr}} \right)^2 \right] \quad (2a)$$

$$K_h = 1 + \frac{\rho_s f_y}{f_c'} \quad (2b)$$

Where f_c is concrete compressive stress, ε_c is concrete strain, f_y is yield strength of transverse reinforcement, ρ_s is ratio of the volume of transverse reinforcement to the volume of concrete core measured to their outer perimeter, and ε_{oc} is the concrete strain at maximum stress ($\varepsilon_{oc} = \varepsilon_o \times K_h$).

After reaching the maximum stress ($\varepsilon_c \geq \varepsilon_{oc} + \varepsilon_{cr}$), the effect of concrete strength and confinement provided by transverse reinforcement were considered by setting the slope of the decaying branch (Z) as a function of concrete confinement, ε_{50u}, and transverse reinforcement confinement, ε_{50h}. ε_{50u} and ($\varepsilon_{50u} + \varepsilon_{50h}$) are the components of the concrete strain measured at a stress of 0.5 $K_h.f_c'$ for unconfined and confined concrete, respectively.

$$Z = \frac{0.5}{\varepsilon_{50u} + \varepsilon_{50h} - \varepsilon_o - \varepsilon_{cr}} \quad (2c)$$

$$\varepsilon_{50u} = \frac{3 + 0.29 f_c'}{145 f_c' - 1000} + \varepsilon_{cr} \quad (2d)$$

$$\varepsilon_{50h} = 0.75 \rho_s \sqrt{\frac{h'}{S_h}} \quad (2e)$$

$$f_c = K_h f_c' \left[1 - Z \left(\varepsilon_c - \varepsilon_{oc} - \varepsilon_{cr} \right) \right] \geq 0.2 K_h f_c' \quad (2f)$$

Where h' is the width of the concrete core measured to outside of the transverse reinforcement and S_h is centre-to-centre spacing of the transverse reinforcement.

The model proposed by Mander et al. [22] accounted for the improvement in strength and ductility due to confinement provided by rectangle and circular hoops.

$$f_c = \frac{f'_{cc} \cdot \frac{\varepsilon_c}{\varepsilon_{oc}} \cdot r}{r - 1 + \left(\frac{\varepsilon_c}{\varepsilon_{oc}}\right)^r} \quad (3a)$$

$$r = \frac{E_{ci}}{E_{ci} - \frac{f'_{cc}}{\varepsilon_{oc}}} \quad (3b)$$

$$\varepsilon_{oc} = \varepsilon_o \cdot \left[1 + 5 \cdot \left(\frac{f'_{cc}}{f'_c} - 1\right)\right] \quad (3c)$$

Where f'_{cc} is the compressive strength of confined concrete.

$$f'_{cc} \text{ for circular sections} = f'_c \cdot \left[-1.254 + 2.254 \cdot \sqrt{1 + \frac{7.94 \cdot f'_l}{f'_c}} - \frac{2.f'_l}{f'_c}\right] \quad (3d)$$

The value of the effective lateral confining stress, f'_l, can be taken equal to $K_e \cdot \frac{2 \cdot f_y.A_s}{d_s.S_h}$.

Where d_s is the diameter of the hoop or the spiral and A_s is its cross sectional area. The confinement effectiveness coefficient, K_e, is the ratio between the area of effectively confined concrete core and the area of concrete within the centerline of the transverse reinforcement.

For rectangular sections, f'_{cc} can be determined from the graph provided by Mander et al. [22] or the equations provided by Akkari and Duan [32] based on the confinement provided in two perpendicular directions (f'_{lx} and f'_{ly}).

The maximum useful strain for confined concrete was defined by Paulay and Priestley [33] as the strain at which the transverse confining steel reaches it ultimate tensile strain.

$$\varepsilon_{cu}(\text{confined concrete}) = \varepsilon_{cu}(\text{unconfined concrete}) + \frac{1.4\ \rho_s\ f_y \varepsilon_{sm}}{K_h\ f'_c} \quad (4)$$

Where ε_{sm} is the steel strain at maximum tensile stress.

3. Tensile Stress-Strain Relationship for Concrete at Normal Temperature

The uniaxial stress-strain relationship for concrete in tension is usually modelled by a linear branch until reaching the cracking stress, f_{cr}. The modulus of elasticity of the linear branch can be

taken equal to E_{ci}. Recommended values for f_{cr} are $0.33\,\lambda\sqrt{f_c'}$ (MPa) for cases of direct tension and $0.60\,\lambda\sqrt{f_c'}$ (MPa) for cases of flexural tension [27]. λ is a factor accounting for the density of the concrete and is equal to 1.00, 0.85, and 0.75 for normal density (density above 2150 kg/m^3), semi-low density (density between 1850 and 2150 kg/m^3), and low density (density below 1850 kg/m^3) concrete, respectively.

After cracking, concrete tensile resistance results from the friction between the concrete and the reinforcing bars and the tensile resistance of the concrete lying between the cracks. One of the popular models to account for tension stiffening in these areas is that of Collins and Mitchell [27].

$$f_t = \frac{\alpha_1\,\alpha_2\,f_{cr}}{1+\sqrt{500\,\varepsilon_c}} \quad (\varepsilon_c > \frac{f_{cr}}{E_{ci}}) \tag{5}$$

Where α_1 is a factor accounting for bond characteristics of reinforcing bars and can be taken equal to 1.0 or 0.7 for deformed or plain reinforcing bars, respectively. α_2 is a factor accounting for type of loading and can be taken equal to 1.0 or 0.7 for short-term or sustained loading, respectively.

4. Concrete Compressive Strength at Elevated Temperature

A number of models exist in the literature that estimates the compressive strength of concrete at elevated temperature, f_{cT}'. These models are based on experimental results of compressive tests done on concrete specimens heated to pre-specified temperatures. Some of the tests involved applying initial compressive stresses on the concrete specimens during heating.

The model of Lie et al. [34] (equation 6) was used by Lin et al. [35] to investigate the behaviour of repaired concrete columns after fire. They concluded that the repaired columns could develop their original strength.

$$f_{cT}' = f_c' \cdot (1 - 0.001 \cdot T) \qquad T \le 500\ ^oC \tag{6a}$$

$$f_{cT}' = f_c' \cdot (1.375 - 0.00175 \cdot T) \qquad 500\ ^oC \le T \le 700\ ^oC \tag{6b}$$

$$f_{cT}' = 0 \qquad T \ge 700\ ^oC \tag{6c}$$

The Eurocode model [36] (equation 7) was used by Saafi [37] to study the effect of fire on concrete members reinforced with Fiber Reinforced Polymers (FRP). The study recommended a minimum concrete cover of 64 mm for FRP reinforced concrete.

$$f'_{cT} = f'_c \qquad T \le 100\ ^oC \tag{7a}$$

$$f'_{cT} = f'_c \cdot (1.067 - 0.00067 \cdot T) \qquad 100\ ^oC \le T \le 400\ ^oC \tag{7b}$$

$$f'_{cT} = f'_c \cdot (1.44 - 0.0016 \cdot T) \quad \ge 0 \qquad T \ge 400\ ^oC \tag{7c}$$

Lie and Lin model [38] (equation 8) was used by Zha [39] to develop a nonlinear finite element program to calculate the resistance of concrete members subjected to fire.

$$f'_{cT} = f'_c \cdot \left(2.011 - 2.353 \cdot \frac{T-20}{1000}\right) \quad \le \quad f'_c \tag{8}$$

Li and Purkiss [40] used their model (equation 9) to provide a comparison between different stress-strain constitutive equations at elevated temperature.

$$f'_{cT} = f'_c \cdot \left[0.00165 \cdot \left(\frac{T}{100}\right)^3 - 0.03 \cdot \left(\frac{T}{100}\right)^2 + 0.025 \cdot \left(\frac{T}{100}\right) + 1.002\right] \tag{9}$$

Hertz [3] proposed a model (equation 10) that recognizes the variation of f'_{cT} with the aggregate type. The decrease in the rate of decay of the concrete strength for preloaded concrete is accounted for by multiplying equation 10 by 1.25 for initial stresses of 0.25 f'_c. This decrease results from the reduction in micro cracking caused by the initial compressive stress and was observed by other researchers [2,4, 6, 7] as well.

$$f'_{cT} = f'_c \cdot \left[\frac{1}{1 + \frac{T}{T_1} + \left(\frac{T}{T_2}\right)^2 + \left(\frac{T}{T_8}\right)^8 + \left(\frac{T}{T_{64}}\right)^{64}}\right] \tag{10}$$

The proposed values for T_1, T_2, T_8, and T_{64} are:

Siliceous aggregate: T_1=15,000, T_2=800, T_8=570, and T_{64}=100,000.

Lightweight aggregate: T_1=100,000, T_2=1100, T_8=800, and T_{64}=940.

Other aggregates: T_1=100,000, T_2=1080, T_8=690, and T_{64}=1000.

Fig. 2a compares the predictions of the above-mentioned models for siliceous aggregate concrete at different temperatures against the experimental results by Malhotra [5], Pettersson

[reported in 4], and Abrams [2]. It is clear that Lie and Lin model [38] and Lie et al. model [34] provide the upper and lower bounds for f'_{cT}. The results of the remaining models [3, 36, 40] are closely correlated. In comparison with the experimental results, all models predicted the decrease in the concrete strength with suitable accuracy considering the high variability of the problem.

Figs. 2b and 2c show the effect of aggregate type on f'_{cT}. Hertz model [3] is found to have good accuracy in predicting the test results provided by Abrams [2] for concrete with carbonate and lightweight aggregates. The remaining models [36, 40] need to be extended to account for the aggregate type.

The experimental results provided by Abrams [2] that shows the effect of initial preload on f'_{cT} are shown in Fig. 3 together with predictions of Hertz model [3]. Even so the initial stress ($0.4\,f'_c$) is higher than that reported by Hertz [3] ($0.25\,f'_c$), a factor of 1.25 is used due to the unavailability of other recommendations. The predictions of Hertz model [3] are found to have good accuracy.

Among the models available in the literature, Hertz model [3] is found to be the most comprehensive, since it accounts for the effect of aggregate type and initial compressive stress on f'_{cT}. Additional experimental work is needed to identify the effect of different levels of initial compressive and tensile stresses on f'_{cT}.

5. Concrete Strain at Elevated Temperature

The concrete strain at elevated temperature consists of four terms: instantaneous stress-related strain (ε_{fT}), unrestrained thermal strain (ε_{th}), and creep strain (ε_{tr}). Definitions and calculations of these strain terms are given below.

5.1. Instantaneous stress related strain

ε_{fT} is a function of the applied stress and the temperature. Its value at the peak stress (ε_{oT}) and the initial value for the Modulus of Elasticity, E_{ciT}, define the shape of the stress-strain curve.

5.1.1. Strain at peak stress at elevated Temperature:

A number of models exist for estimating ε_{oT}. Equations 11 to 15 provide a summary for these models for cases where concrete specimens were not loaded during the heating process.

Lie [4] $$\varepsilon_{oT} = 0.0025 + \left(6.0 \cdot T + 0.04 \cdot T^2\right) \times 10^{-6} \quad (11)$$

Li and Purkiss [40] $$\varepsilon_{oT} = \frac{2 \cdot f_c'}{E_{ci}} + 0.21 \times 10^{-4} \cdot (T - 20) - 0.9 \times 10^{-8} \cdot (T - 20)^2 \quad (12)$$

Lu and Yao [reported in 9] $$\varepsilon_{oT} = \varepsilon_o \cdot (0.0019 \cdot T + 0.9615) \quad (13)$$

Khennane and Baker [10] $$\varepsilon_{oT} = 0.003 \qquad 20 \le T \le 200^oC \quad (14a)$$

$$\varepsilon_{oT} = 0.00001156 \cdot T + 0.000686 \le 0.0082 \qquad T \ge 200^oC \quad (14b)$$

Bazant and Chern [16] $$\varepsilon_{oT} = 0.0000064 \cdot T + 0.00216 \qquad 20 \le T \le 600^oC \quad (15a)$$

$$\varepsilon_{oT} = 0.000015 \cdot T - 0.003 \qquad 600 \le T \le 650^oC \quad (15b)$$

Initial compressive stress was found to reduce the effect of fire temperature on ε_{oT} [13, 14]. Khennane and Baker [10] studied the experimental results provided by Anderberg and Thelandersson [8] and proposed the following equation for concrete having an initial compressive stress during the heating process.

$$\varepsilon_{oT} = 0.00000167 \cdot T + 0.002666 \ge 0.003 \qquad T \le 800^oC \quad (16)$$

Terro's formula [14] (equation 17) accounted for the initial compressive stress level, λ_L, and was based on the experimental results by Schneider [13].

$$\varepsilon_{oT} = \left(50\lambda_L^2 - 15\lambda_L + 1\right) \cdot \varepsilon_{o1} + 20 \cdot \left(\lambda_L - 5\lambda_L^2\right) \cdot \varepsilon_{o2} + 5 \cdot \left(10\lambda_L^2 - \lambda_L\right) \cdot \varepsilon_{o3} \quad (17a)$$

Where $$\varepsilon_{o1} = 2.05 \times 10^{-3} + 3.08 \times 10^{-6} \cdot T + 6.17 \times 10^{-9} \cdot T^2 + 6.58 \times 10^{-12} \cdot T^3 \quad (17b)$$

$$\varepsilon_{o2} = 2.03 \times 10^{-3} + 1.27 \times 10^{-6} \cdot T + 2.17 \times 10^{-9} \cdot T^2 + 1.64 \times 10^{-12} \cdot T^3 \quad (17c)$$

$$\varepsilon_{o3} = 0.002 \quad (17d)$$

Fig. 4a provides a comparison of the above-mentioned models and the experimental results for specimens with zero initial stress. It is clear that while the models of Lie [4] and Li and Purkiss [40] provide the upper bound for ε_{oT}, the model of Lu and Yao [reported in 9] provides the lower bound. The results of the three remaining models are closely related and in good agreement with

the experimental results. The effect of compressive load level that varies between $0.17\,f_c'$ and $0.225\,f_c'$ on ε_{oT} is shown in Fig. 4b. The models of Terro [14] and Khennane and Baker [10] were in good agreement with the experimental results. Among the models available in the literature, Terro's model [14] has the advantage of accounting for different compressive stress levels and providing good accuracy. Additional experiments accounting for different levels of initial compressive and tensile stresses are needed to further validate and improve this model.

5.1.2. Initial Modulus of Elasticity at Elevated Temperature

The modulus of elasticity of the concrete is affected primarily by the same factors influencing its compressive strength [6]. A great scatter in the experimental results for the initial modulus of elasticity was observed by a number of researchers [4, 6, 7, 15]. A summary of the available models is given below.

Lu [reported in 9]

$$E_{ciT} = (1 - 0.0015 \cdot T) \cdot E_{ci} \qquad 20 \le T \le 200^{o}C \qquad (18a)$$

$$E_{ciT} = (0.87 - 0.00084 \cdot T) \cdot E_{ci} \quad \ge 0.28 \cdot E_{ci} \qquad (18b)$$

Li and Guo [reported in 9]

$$E_{ciT} = E_{ci} \qquad 20 \le T \le 60^{o}C \qquad (19a)$$

$$E_{ciT} = (0.83 - 0.0011 \cdot T) \cdot E_{ci} \qquad 60 \le T \le 700^{o}C \qquad (19b)$$

Li and Purkiss [40]

$$E_{ciT} = \frac{800 - T}{740} \cdot E_{ci} \qquad \le E_{ci} \qquad (20)$$

BSI [41]

$$E_{ciT} = \frac{700 - T}{550} \cdot E_{ci} \qquad \le E_{ci} \qquad (21)$$

Schneider [15]

Normal weight concrete:

$$E_{ciT} = (-0.001552 \cdot T + 1.03104) \cdot g \cdot E_{ci} \qquad 20 \le T \le 600^{o}C \qquad (22a)$$

$$E_{ciT} = (-0.00025 \cdot T + 0.25) \cdot g \cdot E_{ci} \qquad 600 \le T \le 1000^{o}C \qquad (22b)$$

Lightweight concrete:

$$E_{ciT} = (-0.00102 \cdot T + 1.0204) \cdot g \cdot E_{ci} \qquad 20 \le T \le 1000^{o}C \qquad (23a)$$

$$\text{where} \quad g = 1 + \frac{f_{ci}}{f_c'} \cdot \frac{T - 20}{100} \qquad \frac{f_{ci}}{f_c'} \le 0.3 \qquad (23b)$$

Khennane and Baker [10] Unloaded Concrete:

$$E_{ciT} = (-0.001282 \cdot T + 1.025641) \cdot E_{ci} \qquad 20 \le T \le 800^{o}C \tag{24}$$

Preloaded Concrete:

$$E_{ciT} = (-0.000634 \cdot T + 1.012673) \cdot E_{ci} \qquad 20 \le T \le 525^{o}C \tag{25a}$$

$$E_{ciT} = (-0.002036 \cdot T + 1.749091) \cdot E_{ci} \qquad 525 \le T \le 800^{o}C \tag{25b}$$

Anderberg and Thelandersson [8]: $$E_{ciT} = \frac{2 \cdot f'_{cT}}{\varepsilon_{oT}} \tag{26}$$

Figs. 5a, 5b and 6 show a comparison between experimental results for E_{ciT} and the predictions of the above models. For Anderberg and Thelandersson model [8], ε_{oT} and f'_{cT} were calculated using Terro [14] and Hertz [3] models, respectively. Considering the significant scatter of the experimental results reported in the literature, all models predicted E_{ciT} for unloaded concrete with acceptable accuracy. Khennane and Barker [10], Schneider [15], and Anderberg and Thelandersson [8] models were the only models that account for the effect of preloading on E_{ciT} with acceptable accuracy. By using Hertz model [3] to predict f'_{cT}, Anderberg and Thelandersson model was having an additional advantage, since it accounts implicitly for the type of aggregates.

5.2. Unrestrained thermal strain

ε_{th} is the free thermal expansion resulting from fire temperature. Traditionally, it is expressed by a linear function of temperature by employing a thermal expansion coefficient, α.

$$\varepsilon_{th} = \alpha \cdot (T - 20\,^{\circ}C) \tag{27}$$

For concrete with siliceous or carbonate aggregates, α can to be taken equal to 18 x 10^{-6} and 12 x 10^{-6} per ^{o}C, respectively, to conduct approximate calculations [7]. Lie [4] proposed using equation 28 for concrete with siliceous or carbonate aggregates to calculate ε_{th} and thus employing a linear function for α.

$$\varepsilon_{th} = (0.008 \cdot T + 6) \times 10^{-6} \times (T - 20^{o}C) \tag{28}$$

Purkiss [7] suggested that ε_{th} is nonlinear with respect to temperature. The nonlinearity results from lack of thermal compatibility between the aggregates and the matrix, and from the chemical and physical changes of the aggregates at elevated temperature. This phenomenon was taken into account in the equations given by Eurocode [36].

Concrete with siliceous aggregates:

$$\varepsilon_{th} = -1.8\times10^{-4} + 9\times10^{-6}\cdot(T-20\,^{\circ}C) + 2.3\times10^{-11}\cdot(T-20\,^{\circ}C)^3 \quad \le 14\times10^{-3} \tag{29}$$

Concrete with carbonate aggregates:

$$\varepsilon_{th} = -1.2\times10^{-4} + 6\times10^{-6}\cdot(T-20\,^{\circ}C) + 1.4\times10^{-11}\cdot(T-20\,^{\circ}C)^3 \quad \le 12\times10^{-3} \tag{30}$$

For concrete with lightweight aggregates, fire temperature was to found to have little effect on the value of α. Lie [4] and Eurocode [36] recommended taking α equal to 7.5 x 10^{-6} and 8 x 10^{-6}, respectively.

Fig. 7 provides a comparison between the predictions of Lie [4] and Eurocode [36] models and the experimental results of Abrams [42], Pettersson [reported in 4], and Khoury [18]. The predictions of both models were closely correlated for concrete with lightweight and carbonate aggregates. For concrete with siliceous aggregates, the predictions of the EuroCode model [36] were having better matching with the experimental results.

5.3. Creep strains:

It was observed that preloaded concrete elements experience a characteristic marked increase in strains during first heating [17-19]. This increase significantly exceeds the expected creep strains [4, 7, 43] and was termed "Transient Creep Strain". Two experimental procedures were used in the literature to evaluate this strain. The first is based on the method used to evaluate creep strains at ambient conditions and it involves heating the test specimen uniformly to a desired temperature. This is followed by applying a constant load and measuring the variation of specimen's strain with time [44]. In the second procedure, the test specimen is subjected to a constant uniaxial compressive load and immediately afterwards heated at a constant rate to a pre-specified temperature [17, 18]. The variation of the specimen's strain with time is recorded starting at the instant of first heating.

The creep strains obtained from the first procedure do not represent the behaviour of concrete structures under fire conditions. During fire, structural elements are being exposed to a variable temperature, which results in a non-uniform and varying temperature distribution within the element. Malhotra [6] recommended using the second test procedure, which was referred to as "short-duration transient-creep tests". The strains measured while using this procedure implicitly include both conventional and transient creep strains [14, 15, 17, 18]. A number of analytical models capable of predicting transient creep strains (ε_{tr}) exist in the literature. They are based on experimental results and are summarized below.

5.3.1. Anderberg and Thelandersson Model [8]:

Transient creep strain was assumed to be proportional to the applied stress and to the thermal strain. This is similar to the assumption made by England [45] where creep strain was proportional to the applied stress and a polynomial expression in temperature.

$$\varepsilon_{tr} = k_{tr} \cdot \left(\frac{f_{cT}}{f_c'}\right) \cdot \varepsilon_{th} \qquad T \le 550\ ^{o}C \tag{31a}$$

$$\frac{\partial \varepsilon_{tr}}{\partial T} = 0.0001 \cdot \left(\frac{f_{cT}}{f_c'}\right) \qquad T \ge 550\ ^{o}C \tag{31b}$$

Where k_{tr} is a constant that varies between 1.8 and 2.35.

Nielsen et al. [46] modified this model by assuming that transient creep strain is linearly proportional with the temperature instead of the thermal strain and by using one equation for the full temperature range (equation 32).

$$\varepsilon_{tr} = 0.000038 \cdot \left(\frac{f_{cT}}{f_c'}\right).T \tag{32}$$

Diederichs model [reported in 40], given by equation 33, is similar in nature to Anderberg and Thelandersson Model [8].

$$\varepsilon_{tr} = \frac{f_{cT}}{f_c'} \cdot \left[3.3 \times 10^{-10} \cdot (T-20)^3 - 1.72 \times 10^{-7} \cdot (T-20)^2 + 0.0412 \times 10^{-3} \cdot (T-20)\right] \tag{33}$$

5.3.2 Schneider's Model [15]:

Transient creep strain was given as a function of corresponding stress (f_{cT}), temperature, initial stress before heating (f_{ci}), and temperature-dependent concrete modulus of elasticity and strength.

$$\varepsilon_{tr} = \frac{\Phi}{g} \cdot \frac{f_{cT}}{E_{ciT}} \tag{34a}$$

$$\Phi = g \cdot \left\{ C_1 \cdot \tanh\left[\gamma_w \cdot (T - 20)\right] + C_2 \cdot \tanh\left[\gamma_o \cdot \left(T - T_g\right)\right] + C_3 \right\} + \frac{f_{cT}}{f'_{cT}} \cdot \frac{T - 20}{100} \tag{34b}$$

Where g is given by equation 23b and $\frac{f_{cT}}{f'_{cT}}$ should not be taken more than 0.3 .

$$\gamma_W = \left(0.3 \cdot w + 2.2\right) \times 10^{-3} \tag{34c}$$

Where w is the moisture content and C_1, C_2, C_3, γ_O , and T_g are constants with values equal to

2.60, 1.40, 1.40, 0.0075, and 700 for concrete with siliceous aggregates,

2.60, 2.40, 2.40, 0.0075, and 650 for concrete with carbonate aggregates, and

2.60, 3.00, 3.00, 0.0075, and 600 for concrete with lightweight aggregates.

5.3.3. Terro's Model [14]:

Terro's model [14] was based on the experimental results by Khoury et al. [18] and accounted for the effect of the volume fraction of aggregates (V_a) on the transient creep strain.

$$\varepsilon_{tr} = \varepsilon_{0.3} \times \left(0.032 + 3.226 \cdot \frac{f_{ci}}{f'_c} \right) \cdot \frac{V_a}{0.65} \qquad \text{where } \frac{f_{ci}}{f'_c} \text{ should not be taken more than } 0.3 \tag{35a}$$

Where $\varepsilon_{0.3}$ is the value of ε_{tr} for initial stress of $0.3 \cdot f'_c$. Its value can be estimated using equations (35b) for concrete with carbonate and lightweight aggregates and equation (35c) for concrete with siliceous aggregates:

$$\varepsilon_{0.3} = -43.87 \times 10^{-6} + 2.73 \times 10^{-8} \cdot T + 6.35 \times 10^{-8} \cdot T^2 - 2.19 \times 10^{-10} \cdot T^3 + 2.77 \times 10^{-13} \cdot T^4 \tag{35b}$$

$$\varepsilon_{0.3} = -1625.78 \times 10^{-6} + 58.03 \times 10^{-6} \cdot T - 0.6364 \times 10^{-6} \cdot T^2 + 3.6112 \times 10^{-9} \cdot T^3 - 9.2796 \times 10^{-12} \cdot T^4 + 8.806 \times 10^{-15} \cdot T^5 \tag{35c}$$

Comparisons between the predictions of presented transient creep models and the experimental results by Fischer [reported in 47], Anderberg and Thelandersson [8], and Kordina et al. [19] are given in Figs. 8a, 8b, and 8c. The experimental results show a nonlinear relationship between the temperature and the transient creep strain. Although the relationship proposed by Nielsen [46] is linear, it agrees well with the experimental results for temperatures less than 500° Celsius. It can be used if simplified calculations are required. Schneider's model [15] provided a lower bound for the results. Models of Anderberg and Thelandersson [8], Terro [14], and Diederichs [reported in 40] were found to provide good accuracy.

5.4. Maximum Compressive Strain at Elevated Temperature

Research in this area is limited. It is expected that the maximum compressive strain for unconfined concrete, ε_{uT}, will decrease with increasing the temperature. Terro [14] proposed to use (equation 1) to calculate ε_{uT} as a function of f'_{cT}.

6. Concrete Tensile Strength at Elevated Temperature:

Research in this area is limited. The tensile resistance of concrete at elevated temperature, f_{crT}, was recommend to be taking equal to $f_{cr}.\frac{f'_{cT}}{f'_c}$ by Terro [14] where f_{cr} was assumed to be equal to $\frac{f'_c}{10}$. Bazant and Chern [16] proposed a model based on the experimental results of Anderberg and Thelandersson [8] to calculate the tensile resistance of concrete at elevated temperature, f_{crT}.

$$f_{crT} = f_{cr} \cdot \left(-0.000526 \cdot T + 1.01052\right) \qquad 20^oC \le T \le 400^oC \qquad (36a)$$

$$f_{crT} = f_{cr} \cdot \left(-0.0025 \cdot T + 1.8\right) \qquad 400^oC \le T \le 600^oC \qquad (36b)$$

$$f_{crT} = f_{cr} \cdot \left(-0.0005 \cdot T + 0.6\right) \qquad 600^oC \le T \le 1000^oC \qquad (36c)$$

Li and Guo [reported in 9] suggested a simpler formula to calculate f_{crT}.

$$f_{crT} = f_{cr} \cdot (1 - 0.001 \cdot T) \qquad 20^{o}C \le T \le 1000^{o}C \qquad (37)$$

Fig. 9 shows a comparison between the predictions of these models and the experimental results of CEB [reported in 4] and Anderberg and Thelandersson [8]. All models predicted a decrease of f_{crT} with temperature. Terro [14] model agrees well with the experimental results. It is also a function of f'_{cT} and thus accounts indirectly for the effect of aggregate type on the tensile resistance. Additional tensile tests at elevated temperature are needed to validate this model.

7. Yield Stress of Reinforcing Bars at Elevated Temperature

Elevated temperatures reduce the yield strength of the reinforcing bars and eliminate the yielding plateau observed in tensile tests of mild steel specimens. Due to large strains exhibited at elevated temperature, the yield strength (f_{yT}) is usually evaluated using the 1.0% or 2.0% proof stress rather than the conventional ambient value of 0.2% [7]. Two of the available models to predict yield stress, f_{yT}, of reinforcing bars at elevated temperature are given below.

Lie [4]

$$f_{yT} = \left[1 + \frac{T}{900 \cdot \ln\left(\frac{T}{1750}\right)}\right] \cdot f_y \qquad 0 < T \le 600\ ^{o}C \qquad (38a)$$

$$f_{yT} = \left[\frac{340 - 0.34 \cdot T}{T - 240}\right] \cdot f_y \qquad 600 < T \le 1000\ ^{o}C \qquad (38b)$$

Lie and Stanzak [48]

$$f_{yT} = f_y\left(1 - 0.78 \cdot T^{*} - 1.89 \cdot T^{*4}\right) \qquad (39a)$$

$$T^{*} = \frac{\left(\frac{9}{5} \cdot T - 36\right)}{1800} \qquad (39b)$$

Fig. 10 shows a comparison between the predictions of these models, the Eurocode [36] recommended curve for f_{yT} and the available experimental results. Predictions of Lie [4] model were found to have good accuracy and it can be easily incorporated in a finite element code.

8. Bond Strength of Reinforcing Bars at Elevated Temperature

Bond strength between the concrete and steel decreases with increasing temperature. The magnitude of the loss is a function of the type of concrete and the reinforcement surface's condition (smooth, deformed, degree of rusting) [7]. Deformed or plain bars with rusted surface show higher bond strength at high temperatures than smooth plain bars [6]. Models predicting the bond strength at elevated temperature, τ_{uT}, are limited. Xie and Qian Model [reported in 9] proposed equation 40 to calculate τ_{uT} as a function of the bond strength at ambient temperature, τ_{uo}, and the temperature of the reinforcing bar, T. Fig. 11 shows the predictions given by this model against the available experimental results. The scatter observed in the experimental results might be due to no uniformity in test procedures [6].

$$\tau_{uT} = \tau_{uo} \cdot \left[2.7438 \cdot \left(\frac{T}{100} \right)^2 - 3.322 \cdot \left(\frac{T}{10} \right) + 105.881 \right] \times 10^{-2} \qquad (40)$$

9. Concrete Stress-Strain Relationships at Elevated Temperature:

This section summarizes the existing stress-strain relationships for concrete at elevated temperature and provides a description of the proposed relationships. The formulations that were recommended in the previous sections will be used to calculate the parameters affecting the stress-strain relationships. These are equation 10 by Hertz [3] for concrete compressive strength (f'_{cT}), equation 17 by Terro [14] for strain at peak stress (ε_{oT}), equation 1 as a function of f'_{cT} by Terro [14] for maximum compressive strain, $f_{cr} \cdot \frac{f'_{cT}}{f'_c}$ by Terro [14] for concrete tensile strength, equation 26 by Anderberg and Thelandersson [8] for initial concrete modulus of elasticity, equations 29 and 30 by Eurocode [36] for unrestrained thermal strain, equation 38 by Lie [4] for yield strength of reinforcing bars (f_{yT}), equation 40 by Xie and Qian [reported in 9] for bond strength (τ_{uT}), and any of equations 31, 33, or 35 by Anderberg and Thelandersson [8], Diederichs [reported in 40], and Terro [14], respectively, for transient creep strains (ε_{tr}). These recommended formulations would be utilized in this section.

9.1 Compressive Stress-Strain relationship

Few models describing the compressive stress-strain relationship of unconfined concrete at elevated temperature exist in the literature. Lie and Lin [38] proposed an instantaneous stress-strain relation for concrete with parabolic ascending and descending branches.

$$f_{cT} = f'_{cT} \cdot \left[1 - \left(\frac{\varepsilon_{oT} - \varepsilon_{cT}}{\varepsilon_{oT}} \right)^2 \right] \qquad \varepsilon_{cT} \le \varepsilon_{oT} \qquad (41a)$$

$$f_{cT} = f'_{cT} \cdot \left[1 - \left(\frac{\varepsilon_{cT} - \varepsilon_{oT}}{3\varepsilon_{oT}} \right)^2 \right] \qquad \varepsilon_{cT} \ge \varepsilon_{oT} \qquad (41b)$$

Anderberg and Thelandersson [8] relationships are parabolic for the ascending branch and linear for the descending branch.

$$f_{cT} = E_{ciT} \cdot \left[\varepsilon_{cT} - \frac{\varepsilon_{cT}^2}{2 \cdot \varepsilon_{oT}} \right] \qquad \varepsilon_{cT} \le \varepsilon_1$$

(42a)

$$f_{cT}\,(\text{MPa}) = f_1\,(\text{MPa}) - 880 \cdot (\varepsilon_{cT} - \varepsilon_1) \qquad \varepsilon_1 \le \varepsilon_{cT} \qquad (42b)$$

$$f_1 = E_{ciT} \cdot \left(\varepsilon_1 - \frac{\varepsilon_1^2}{2 \cdot \varepsilon_{oT}} \right) \qquad (42c)$$

$$\varepsilon_1 = \varepsilon_{oT} \cdot \left(1 - \frac{880\,\text{MPa}}{E_{ciT}} \right) \qquad (42d)$$

Schneider [15] proposed a model that accounts concrete weight on the shape of the stress-strain curve by using a non-dimensional factor n. Its value was recommended to be taken equal to 2.5 and 3.0 for lightweight and normal-weight concrete, respectively.

$$\varepsilon_{cT} = \left[1 + \frac{1}{n-1} \cdot \left(\frac{\varepsilon_{cT}}{\varepsilon_{oT}} \right)^n \right] \cdot \frac{f_{cT}}{E_{ciT}} \qquad (43)$$

Terro [14] recommended using n equal 2 in Schneider model [15], which makes the model similar to the model of Mander et al. [22] for E_{ci} equal to $\frac{2 \cdot f'_{cT}}{\varepsilon_{oT}}$.

To account for transient creep effects, Anderberg and Thelandersson [8], Schneider [15], Diedrichs [reported in 40], and Terro [14] considered that the total strain is composed of separate strain components. The thermal strain is a function of the temperature and thus can be separated

easily from the total strain. To calculate the transient creep strain, an assumption has to be made for the corresponding stress. This leads to an iterative solution.

9.2 Tensile Stress-Strain relationship

Research addressing the tensile stress-strain relationship for concrete at elevated temperature is limited. A linear relationship is widely used to represent the pre-cracking behaviour. After cracking, Terro [14] suggested using a linear degrading branch that joins the point of cracking and a point on the horizontal axis with a strain of 0.004. Fracture toughness is often utilized to define the softening branch. Zhang and Bicanic [49] assessed the residual fracture toughness of cooled concrete after heating to 600^{o}C. Similar research is needed to assess the fracture toughness of concrete after heating to different temperatures and before cooling.

9.3 Proposed compressive stress-strain relationship

In this section two models are proposed. They are based on the models of Mander et al. [22] and Scott et al. [29]. These models are proved to be successful in modelling the behaviour of concrete at ambient temperature. The models are modified by replacing $f_c^{'}$ and ε_{oc} with the temperature dependent terms $f_{cT}^{'}$ and ε_{oTc}. Transient creep is modelled by shifting the strain at maximum stress by the transient creep strain similar to the approach proposed by Collins and Mitchell [27]. This will remove the requirement for the iterations mentioned in section 9.1 and thus will simplify the implementation of this model in a finite element code.

9.3.1 Analytical model number 1:

The modified Scott et al.'s model is given by the following equations. It is proposed to consider the change in the strain ε_{50u} (Fig. 1a) proportional to the change in ε_o.

$$f_{cT} = K_{hT}\, f'_{cT}\left[2.0\left(\frac{\varepsilon_{cT}}{\varepsilon_{oTc}+\varepsilon_{tr}}\right)-\left(\frac{\varepsilon_{cT}}{\varepsilon_{oTc}+\varepsilon_{tr}}\right)^2\right] \qquad \varepsilon_{cT} \le \varepsilon_{oTc} + \varepsilon_{tr} \qquad (44a)$$

$$f_{cT} = K_{hT}\, f'_{cT}\left[1 - Z(\varepsilon_{cT} - \varepsilon_{oTc} - \varepsilon_{tr})\right] \ge 0.2K_{hT}f'_{cT} \qquad \varepsilon_{cT} \ge \varepsilon_{oTc} + \varepsilon_{tr} \qquad (44b)$$

$$K_{hT} = 1 + \frac{\rho_s\, f_{yT}}{f'_{cT}} \qquad (44c)$$

$$\varepsilon_{oTc} = \varepsilon_{oT} \text{ x } K_{hT} \qquad (44d)$$

$$Z = \frac{0.5}{\varepsilon_{50uT} + \varepsilon_{50h} - \varepsilon_{oTc} - \varepsilon_{tr}} \qquad (44e)$$

$$\varepsilon_{50uT} = \frac{3 + 0.29 f'_c}{145 f'_c - 1000}.\frac{\varepsilon_{oTc}}{\varepsilon_{oc}} + \varepsilon_{tr} \qquad (44f)$$

9.3.2 Analytical model number 2:

The modified Mander et al.'s model is given by the following equations. It is proposed to use E_{ci} equal to $\frac{2 \cdot f'_{cT}}{\varepsilon_{oT}}$ and thus r will be equal to 2.

$$f_{cT} = \frac{2.f'_{ccT} \cdot \varepsilon_{cT}}{(\varepsilon_{ocT} + \varepsilon_{tr}).\left[1 + \left(\frac{\varepsilon_{cT}}{\varepsilon_{ocT} + \varepsilon_{tr}}\right)^2\right]} \qquad (45a)$$

$$\varepsilon_{ocT} = \varepsilon_{oT} \cdot \left[1 + 5 \cdot \left(\frac{f'_{ccT}}{f'_{cT}} - 1\right)\right] \qquad (45b)$$

$$f'_{ccT} \text{ for circular sections} = f'_{cT} \cdot \left[-1.254 + 2.254 \cdot \sqrt{1 + \frac{7.94 \cdot f'_{lT}}{f'_{cT}}} - \frac{2.f'_{lT}}{f'_{cT}}\right] \qquad (45c)$$

The value of f'_{lT} can be taken equal to $K_e \cdot \frac{2 \cdot f_{yT}.A_s}{d_s.S_h}$. For rectangular sections, f'_{ccT} can be determined from the graph provided by Mander et al. [22] or equations provided by Akkari and Duan [32] based on the area of stirrups and their temperature dependent yield strength provided in two perpendicular directions (f'_{lxT} and f'_{lyT}).

9.4 Proposed tensile stress-strain relationship

The uniaxial stress-strain relationship for concrete in tension can be modelled by a linear branch until reaching the cracking stress, f_{crT}. The modulus of elasticity of the linear branch can be taken equal to E_{ciT}. Recommended values for f_{crT} are $\left(0.33 \lambda \sqrt{f_c^{'}} \right).\frac{f_c^{'}}{f_{cT}^{'}}$ (MPa) for cases of direct tension and $\left(0.60 \lambda \sqrt{f_c^{'}} \right)\frac{f_c^{'}}{f_{cT}^{'}}$ (MPa) for cases of flexural tension. After cracking, the model of Collins and Mitchell [27] can be modified by accounting for the reduction in the tensile resistance and the bond strength.

$$f_{tT} = \frac{\alpha_1 \alpha_2 f_{crT}}{1+\sqrt{500 \varepsilon_{cT}}}.\frac{\tau_{uT}}{\tau_{uo}} \quad (\varepsilon_{cT} > \frac{f_{crT}}{E_{ciT}} \quad) \tag{46}$$

9.5 Comparisons

A Comparison between different instantaneous stress-strain models and the experimental results of Purkiss and Dougill [11], Bazant and Chern [16], and Schneider [55] is given in Fig. 12. In the figure, the modified Scott et al.'s model is referred as "Analytical 1" and the modified Mander et al.'s model is referred as "Analytical 2". For all models, $f_{cT}^{'}$ and ε_{oT} were calculated using the formulations proposed by Hertz [3] and Terro [14], respectively. The predictions of the models of Terro [14] and Schneider [15] were matching those represented by the modified Mander et al.'s model for n equal to 2. All models represented the ascending branch with good accuracy. The modified Scott et al.'s model provided the most accurate predictions for the descending branch at different temperatures.

Due to the unavailability of the experimental data providing the full stress-strain curve including transient creep effect, a comparison between different analytical models is given in Fig. 13. It was assumed that f_{ci}=0.2 $f_c^{'}$. The model of Anderberg and Thelandersson [8] was used to calculate transient creep strains for the proposed models. The ascending branches for all models with the exception of Terro's model [14] are almost matching. This mainly due to the high values of

transient creep strains used in Terro's model [14]. High variability exists in the predictions of the descending branches. This requires experimental results to confirm the suitability of the proposed models.

Figs. 14, 15, and 16 provide a comparison between the different models and the experimental results provided by Terro and Hamoush [56] for compression tests on unconfined and confined concrete cylinders. For unconfined concrete (Fig. 14), the ascending branches of Anderberg and Thelandersson [8], Lie [4], and the modified Scott et al. models coincided. Also, those of Schneider [15], Terro [14], and Mander [22] models coincided. The predictions of all models were almost matching and were in good agreement with the experimental results. For confined concrete cylinders, two confinement ratios (6 rings and 9 rings of high strength steel bars) were used. From figs. 15 and 16, it can be noted that while all models predicted the ascending branch with good accuracy, the modified Scott et al's model and the modified Mander's model were superior in predicting the post peak behaviour.

10. Summary and Conclusions

The mechanical properties of concrete and reinforcing bars that affects the stress-strain relationship of confined concrete are concrete strength, concrete initial modulus of elasticity, concrete strain at maximum stress, thermal strain, transient creep strain, yield strength of reinforcing bars, and bond strength of reinforcing bars. They experience significant changes at elevated temperature. Concrete strength, concrete initial modulus of elasticity, yield strength of reinforcing bars, and bond strength of reinforcing bars decrease while the absolute value of concrete strain at peak stress increases. Initial compressive stresses reduce the effect of elevated temperature on concrete strength and concrete strain at the peak stress but increases transient creep strains. In this paper, comparisons between the predictions of available formulations to estimate concrete and reinforcing bars mechanical properties at elevated temperature and available experimental data were conducted. Specific formulations were recommended for different parameters based on accuracy, generality, and simplicity, or unavailability of other models.

Stress-strain relationships describing the compressive and tensile behaviour of concrete and utilizing the proposed formulations for estimating the mechanical properties of concrete and

reinforcing bars at elevated temperature are proposed. For the compressive behaviour, two models are proposed; both are based on well-established models at ambient temperature. The proposed models capture the changes that occur in the mechanical properties of concrete due to confinement effects and high temperature. They also take into consideration transient creep using a simplified but sufficiently accurate method. To model the stress-strain relationship for concrete in tension, it is proposed to use a linear branch until reaching the cracking stress and after cracking an existing tension softening model was modified by accounting for the reduction in the tensile resistance of concrete and in the bond resistance of the reinforcing bars. The proposed compressive models were found to have good accuracy when their predictions were compared against the available experimental results.

The paper stressed on the fact that additional tests at different temperatures are needed to investigate the role of initial compressive and tensile stresses on concrete compressive strength, concrete strain at peak stress, and initial modulus of elasticity of concrete. Tests are also required to evaluate the effect of elevated temperature on the: maximum compressive concrete strain, tensile behaviour of concrete, bond strength of reinforcing bars, and stress-strain curve for confined initially stressed concrete.

Acknowledgement

This research was funded by the Natural Sciences and Engineering Research Council of Canada (NSERC).

References

[1] Phan LT, Carino NJ. Review of Mechanical Properties of HSC at Elevated Temperature. ASCE Journal of Materials in Civil Engineering 1998; 10(1): 58-64.
[2] Abrams MS. Compressive Strength of Concrete at Temperatures to 1600°F. Temperature and Concrete (Special Publication American Concrete Institute) 1971;SP-25:33-59. Detroit, MI.
[3] Hertz KD. Concrete strength for fire safety design. Mag Concrete Res 2005;57(8):445-53.
[4] Lie TT. Structural Fire Protection. New York: American Society of Civil Engineers; 1992.
[5] Malhotra HL. Effect of Temperature on the Compressive Strength of Concrete. Mag Concrete Res 1956; 8:85-94.
[6] Malhotra HL. Design of Fire-Resisting Structures. London: Surrey University Press; 1982
[7] Purkiss JA. Fire Safety Engineering Design of Structures. Oxford: Butterworth Heinemann; 1996.
[8] Anderberg Y, Thelandersson S. Stress and Deformation Characteristics of Concrete at High Temperatures: 2 Experimental Investigation and Material Behaviour Model. Bulletin 54. Sweden, Lund: Lund Institute of Technology 1976.
[9] Xiao J, Konig G. Study on Concrete at High Temperature in China an Overview. Fire Safety J 2004; 39: 89-103.
[10] Khennane A, Baker G. Uniaxial Model For Concrete Under Variable Temperature and Stress. J Eng Mech-ASCE 1993; 119(8): 1507-25.
[11] Purkiss JA, Dougill JW. Apparatus for Compression Tests on Concrete at High Temperatures. Mag Concrete Res 1973; 25(83): 102-8.
[12] Schneider U. Behavior of Concrete under Thermal Steady State and Non-Steady State Conditions. Fire Mater 1976; 1(3): 103-15.
[13] Schneider U. Properties of Material at High Temperatures-Concrete. RILEM-Committee 44-PHT. Department of Civil Engineering, University of Kassel; 1985.
[14] Terro MJ. Numerical Modeling of the Behavior of Concrete Structures in Fire. ACI Struct J 1998; 95(2): 183-93.
[15] Schneider U. Modelling of Concrete Behaviour at High Temperatures. In: Anchor RD, Malhotra HL, Purkiss JA. Proceeding of International Conference of Design of Structures against Fire. 1986. p. 53-69
[16] Bazant P, Chern JC. Stress-Induced Thermal and Shrinkage Strains in Concrete. J Eng Mech-ASCE 1987; 113(10): 1493-1511.
[17] Khoury GA, Grainger BN, Sullivan PJE. Transient Thermal Strain of Concrete Literature Review Conditions Within Specimen and Behaviour of Individual Constituents. Mag Concrete Res 1985; 37(132): 131-144.
[18] Khoury GA, Grainger BN, Sullivan PJE. Strain of Concrete during First Heating to 600 °C under Load. Mag Concrete Res 1985; 37(133): 195-215.
[19] Kordina K, Wydra W, Ehm C. Analysis of the Developing Damage of Concrete Due to Heating and Cooling. In: Harmathy TZ, editor. Symposium of Evaluation and Repair of Fire Damage to Concrete. 1986. p. 87-113.
[20] Felicetti R, Gambarova PG. Effects of High Temperature on the Residual Compressive Strength of High-Strength Siliceous Concretes. ACI Mater J 1998; 95(4): 395-406.
[21] Park R., Paulay T. Reinforced Concrete Structures. New York: John Wiley & Sons; 1975.
[22] Mander JB, Priestley MJN, Park R, Theoretical Stress-Strain Model for Confined Concrete. J Struct Eng-ASCE 1988; 114(8):1804-25.
[23] MacGregor JG, Bartlett FM. Reinforced Concrete Mechanics and Design. Scarborough Ontario: Prentice Hall; 2000.
[24] ACI 318-05 Building Code Requirements for Structural Concrete and Commentary, 2005.
[25] CSA Standard A23.3-04. Concrete Design Handbook. Cement Association of Canada; 2004.
[26] Neville AM. Properties of Concrete, Essex: Longman Scientific and Technical; 1987.
[27] Collins MP, Mitchell D. Prestressed Concrete Basics, Ottawa, ON, Canada: Canadian Prestress Concrete Institute; 1987.
[28] Kent DC, Park R. Flexural Members with Confined Concrete. J Struct Eng-ASCE 1971; 97(ST7): 1969-90.
[29] Scott BD, Park R, Priestley MJN. Stress-Strain Behavior of Concrete Confined by Overlapping Hoops at Low and High Strain Rates. ACI J 1982;79(1):13-27.
[30] Karsan ID, Jirsa JO. Behavior of Concrete under Compressive Loadings. J Struct Eng-ASCE 1969; 95(ST12): 2543-63.

[31] Sheikh SA, Uzumeri SM. Strength and Ductility of Tied Concrete Columns. J Struct Eng-ASCE 1980; 106(5): 1079-102.
[32] Akkari M, Duan L. Chapter 36:Nonlinear Analysis of Bridge Structures. Bridge Engineering Handbook. Edited by Chen WF, Duan L. Boca Raton: CRC Press;2000.
[33] Paulay T, Priesley MJN. Seismic Design of Reinforced Concrete and Masonry Buildings, New York: John Wiley & Sons Inc; 1992.
[34] Lie TT, Rowe TJ, Lin TD. Residual Strength of Fire Exposed RC Columns Evaluation and Repair of Fire Damage to Concrete. American Concrete Institute 1986;SP-92: 153-74. Detroit.
[35] Lin CH, Chen ST, Yang CA. Repair of Fire Damaged Reinforced Concrete Columns. ACI Struct J 1995; 92(4): 406-11.
[36] Eurocode 2: Design of Concrete Structures ENV EC2, 1992.
[37] Saafi M. Effect of fire on FRP Reinforced Concrete Members. Compos Struct 2002; 58:11-20.
[38] Lie TT, Lin TD. Fire Performance of Reinforced Concrete Columns. Fire Safety Science and Engineering ASTM 1985;Paper No.1352: 176-205
[39] Zha XX. Three-Dimensional Non-Linear Analysis of Reinforced Concrete Members in Fire. Build Environ 2003; 38:297-307.
[40] Li L, Purkiss JA. Stress-Strain Constitutive Equations of Concrete Material at Elevated Temperatures. Fire Safety J 2005; 40:669-86.
[41] BSI: Structural Use of Concrete. British Standards Institution. BS 8110; 1985.
[42] Abrams M. S. Behaviour of Inorganic Materials in Fire. ASTM Symposium on Design of Buildings for Fire Safety (Special publication 685). 1978. Boston MA.
[43] Thelandersson S. Modeling of Combined Thermal and Mechanical Action in Concrete. J Eng Mech 1987; 113(6): 893-906.
[44] Gillen M. Short-term Creep of Concrete at Elevated Temperatures. Fire Mater 1981;5(4):142-48.
[45] England GL. Analyses for Creep in Heated Concrete Structures. Report No. CE 75-3. Canada: Department of Civil Engineering, University of Calgary; 1975.
[46] Nielsen CV, Pearce CJ, Bicanic N. Theoretical Model of High Temperature Effects on Uniaxial Concrete Member Under Elastic Restraint. Mag Concrete Res 2002; 54(4): 239-49.
[47] Persson B. Self-Compacting Concrete at Fire Temperature. TVBM-3110. Sweden, Lund: Division of building materials, Lund Institute of Technology; 2003.
[48] Lie TT, Stanzak WW. Empirical Method for Calculating Fire Resistance of Protected Steel Columns. Eng J AISC (Transactions of the Canadian Society for Civil Engineering) 1974; 57.
[49] Zhang B, Bicanic N. Residual Fracture Toughness of Normal- and High-Strength Gravel Concrete after Heating to 600°C. ACI Mater J 2002; 99(3): 217-26.
[50] Cruz CR. An Optical Method of Determining the Elastic Constants of Concrete. Journal of the Portland Cement Association Research and Development Laboratories May 1962:24-32.
[51] Philleo R. Some Physical Properties of Concrete at High Temperatures. Proceedings of the American Concrete Institute 1958; 54:857-64.
[52] Lie TT. Fire and Buildings. London: Applied Science Publishers Ltd; 1972.
[53] Holmes M, Anchor RD, Cook GME, Crook RN. The Effect of Elevated Temperatures on the strength Properties of Reinforcing and Prestressing Steels. Struct Eng 1982; 60B(1): 7-13.
[54] Harmathy TZ, Stanzak WW. Elevated-Temperature Tensile and Creep Properties of Some Structural and Prestressing Steels. American Society for Testing and Materials (Special Technical Publication) 1970; 464:186-208
[55] Schneider U. Behavior of Concrete at High Temperatures. Berlin: Deutscher Ausschuss fur Stahlbeton 1982; 337.
[56] Terro MJ, Hamoush SA. Effect of Confinement on Siliceous Aggregate Concrete Subjected to Elevated Temperatures and Cyclic Heating. ACI Mater J 1997; 94(2): 83-89.

Nomenclature

A_s	Cross sectional area of transverse reinforcement.
C_1, C_2, C_3	Constants to account for aggregate type in evaluating transient creep strain [14].
d_s	Diameter of the transverse reinforcing bars.
E_{ci}	Initial modulus of elasticity at ambient temperature.
E_{ciT}	Initial modulus of elasticity at elevated temperature.
f_1	Stress at the point of intersection of the two equations defining the stress strain curve of concrete [7].
f_c	Concrete compressive stress at ambient temperature.
f'_c	Concrete compressive strength at ambient temperature.
f'_{cc}	Compressive strength of confined concrete at ambient temperature.
f'_{ccT}	Compressive strength of confined concrete at elevated temperature.
f_{ci}	Initial compressive stress before heating.
f_{cr}	Cracking stress of concrete.
f_{crT}	Tensile resistance of concrete at elevated temperature.
f_{cT}	Concrete compressive stress at elevated temperature.
f'_{cT}	Concrete compressive strength at elevated temperature.
f'_l	Effective lateral confining stress at ambient temperature.
f'_{lx}	Effective lateral confining stress in the principal x-direction at ambient temperature.
f'_{ly}	Effective lateral confining stress in the principal y-direction at ambient temperature.
f'_{lT}	Effective lateral confining stress at elevated temperature.
f'_{lxT}	Effective lateral confining stress in the principal x-direction at elevated temperature.
f'_{lyT}	Effective lateral confining stress in the principal y-direction at elevated temperature.
f_t	Concrete tensile stress at ambient temperature.
f_y	Yield strength of reinforcing bars at ambient temperature.
f_{yT}	Yield strength of reinforcing bars at elevated temperature.
g	Function to account for increase in modulus of elasticity due to external loads [14].
h'	Width of the concrete core measured to outside of the transverse reinforcement.
K_e	Confinement effectiveness coefficient.
K_h	Confinement factor at ambient temperature.
K_{hT}	Confinement factor at elevated temperature.
k_{tr}	Constant (1.8 to 2.35) used to evaluate transient creep strain [7].
n	A non-dimensional factor that accounts for effect of the weight of concrete on the shape of the stress-strain curve [14].
r	Ratio between the initial tangent modulus of elasticity of concrete and its difference from the secant modulus at peak stress [20].
S_h	Center-to-center spacing of the transverse reinforcement.
T	Fire temperature in degree Celsius ($\geq 20\ ^oC$).
T_1, T_2, T_8, T_{64}	Constants describing the reduction in the concrete compressive strength for different aggregate types [2].
T_g	Constant to account for aggregate type in evaluating transient creep strain [14].
V_a	Volume fraction of aggregate used to evaluate the transient creep strain [13].
w	Moisture content in percent by weight.
Z	Slope of the decaying branch of the concrete stress-strain curve [26].
α	Coefficient of thermal expansion of concrete.

α_1	Factor to account for bond characteristics of reinforcing bars on the concrete tension stiffening.
α_2	Factor to account for type of loading on the concrete tension stiffening.
γ_o	Constant to account for aggregate type in evaluating transient creep strain [14].
γ_w	Function to account for the effect of moisture content on transient creep strain [14].
ε_c	Concrete strain at ambient temperature.
ε_{cT}	Concrete strain at elevated temperature.
ε_{cr}	Creep strain of concrete at maximum stress.
ε_{cu}	Ultimate or maximum strain of concrete.
ε_{fT}	Instantaneous stress-related strain at elevated temperature.
ε_o	Strain at maximum stress for unconfined concrete at ambient temperature.
ε_{oc}	Strain at maximum stress for confined concrete at ambient temperature.
ε_{o1}, ε_{o2}, ε_{o3}	Strain at maximum stress as function of temperature for 0%, 10%, and 20% initial stress level [13].
ε_{oT}	Strain at maximum stress of unconfined concrete at elevated temperature.
ε_{oTc}	Strain at maximum stress of confined concrete at elevated temperature.
ε_{sm}	Steel strain at maximum tensile stress.
ε_{th}	Unrestrained thermal strain.
ε_{tr}	Transient creep strain.
ε_{uT}	Maximum compressive strain for unconfined concrete at elevated temperature.
$\varepsilon_{0.3}$	Transient creep strain for initial stress of $0.3\,f_c^{'}$ [13].
ε_1	Strain at point of intersection of the two equations defining the stress strain curve of concrete [7].
ε_{20c}	Concrete strain corresponding to a stress equal to 0.2 of the concrete strength at ambient temperature [26].
ε_{20cT}	Concrete strain corresponding to a stress equal to 0.2 of the concrete strength at elevated temperature.
ε_{50h}	Strain component that gives the additional ductility due to rectangular transverse reinforcement [26].
ε_{50u}	Strain component that takes into account effect of concrete strength on the slope of the descending branch of unconfined concrete at ambient temperature [26].
ε_{50uT}	Strain component that takes into account effect of concrete strength on the slope of the descending branch of unconfined concrete at elevated temperature.
λ	Factor accounting for the density of the concrete.
λ_L	Factor accounting for the initial compressive stress level [13].
ρ_s	Ratio of the volume of transverse reinforcement to the volume of concrete core measured to outside of the transverse reinforcement.
Φ	Function to evaluate transient creep strain [14].
τ_{uo}	Bond strength at ambient temperature.
τ_{uT}	Bond strength at elevated temperature.

List of Figures:

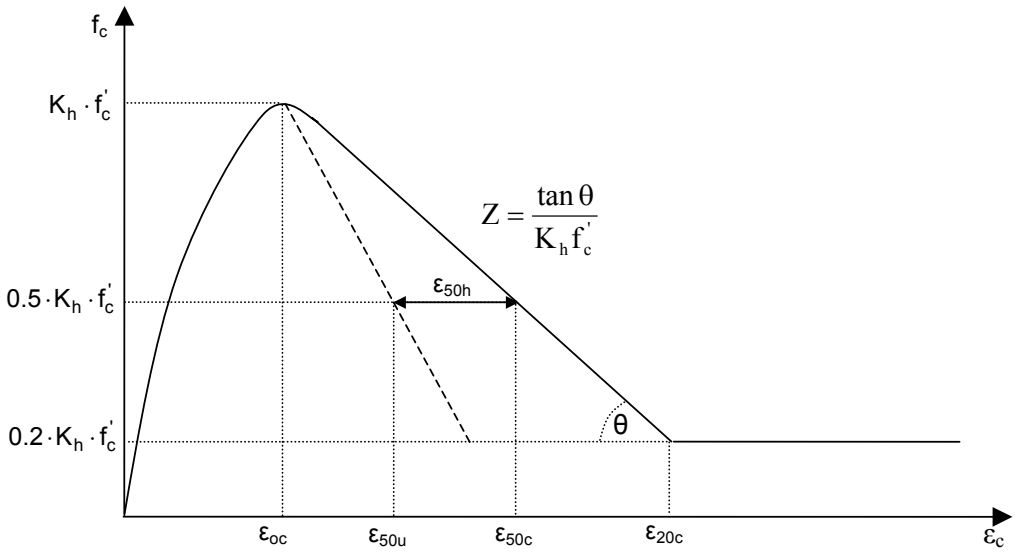

(a) Kent and Park [28].

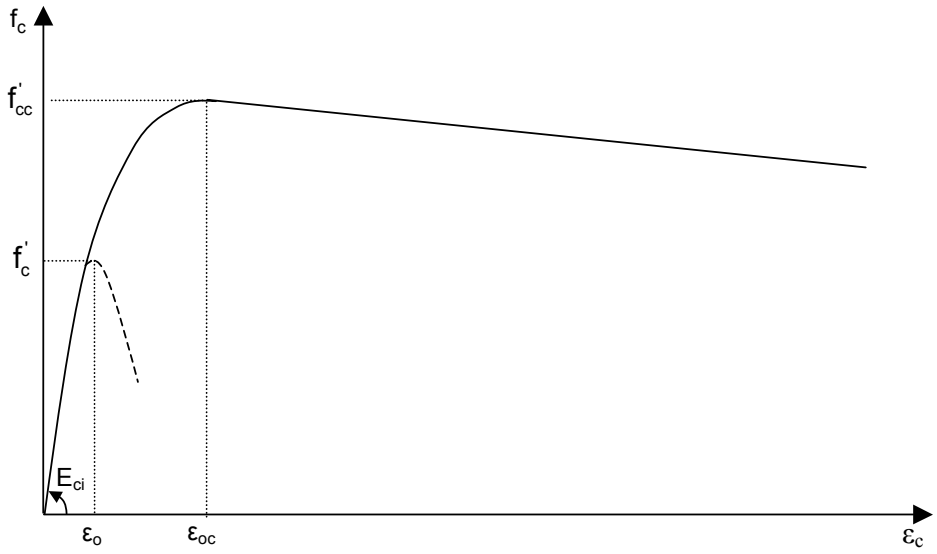

(b) Mander et al. [22].

Fig. 1. Instantaneous stress-strain curve for concrete at ambient temperature.

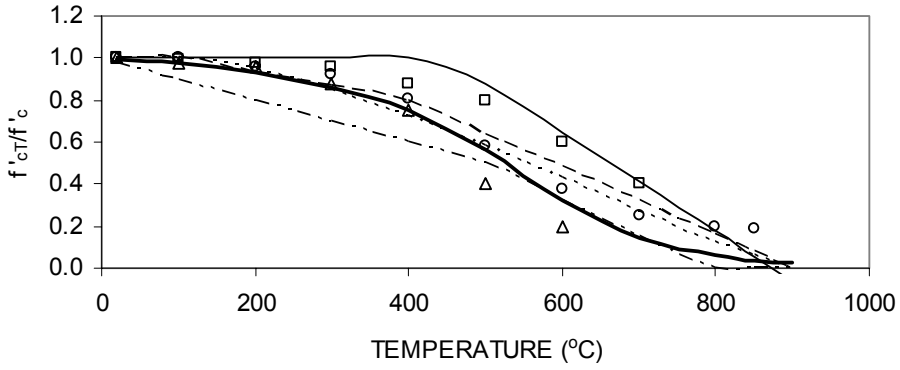

□ Lie (Test) [4] △ Malhotra (Test) [5] ○ Abrams (Test) [2]

(a) Concrete with siliceous aggregates.

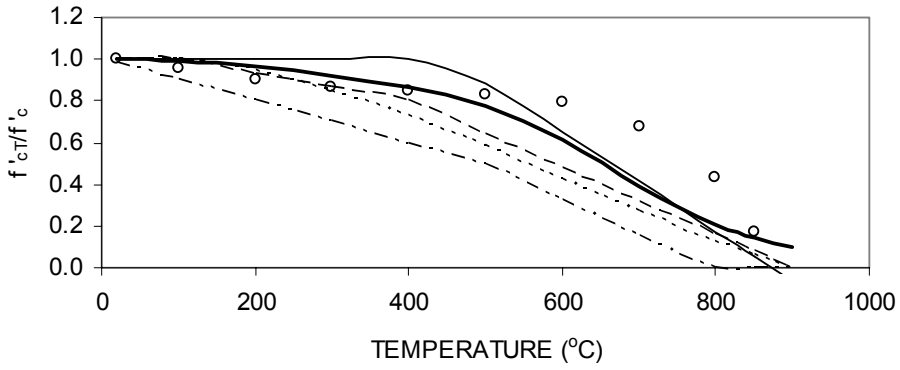

○ Abrams (Test) [2]

(b) Concrete with carbonate aggregates.

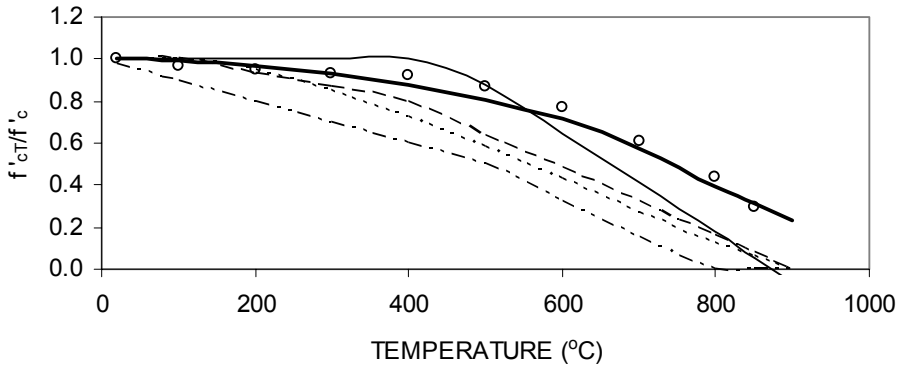

○ Abrams (Test) [2]

(c) Concrete with lightweight aggregates.

Lie, Rowe & Lin (Model) [34] — Eurocode 2 (Model) [36]
Lie & Lin (Model) [38] ····· Li & Purkiss (Model) [40]
Hertz (Model) [3]

Fig. 2. Temperature-compressive strength relationship.

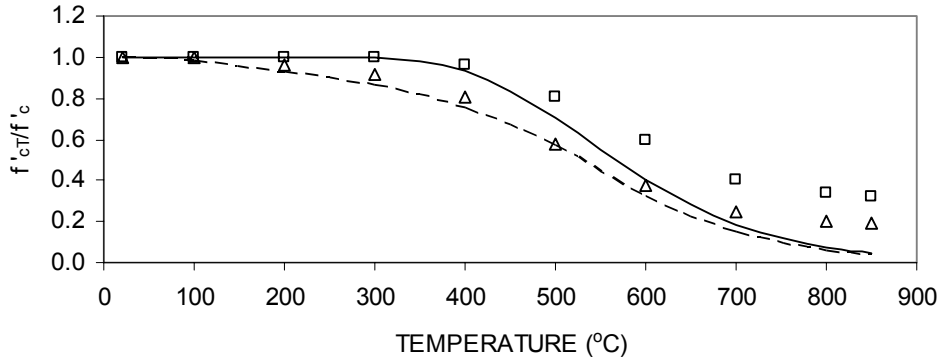

(a) Concrete with siliceous aggregates.

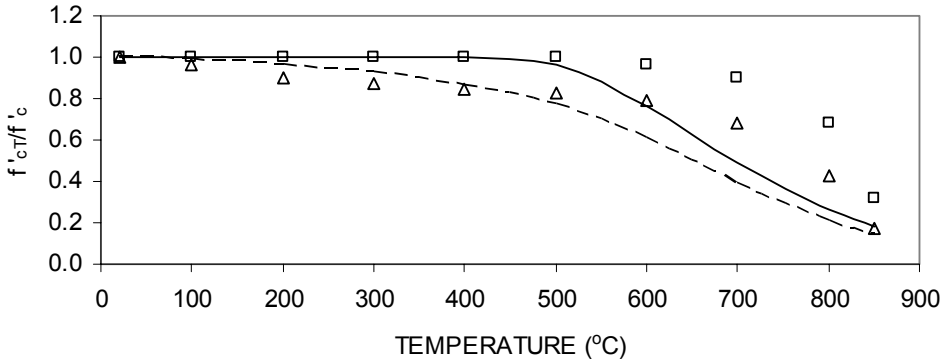

(b) Concrete with carbonate aggregates.

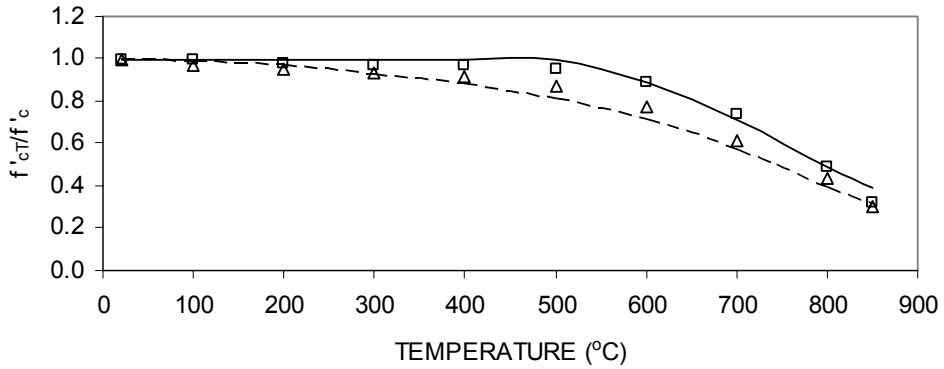

(c) Concrete with lightweight aggregates.

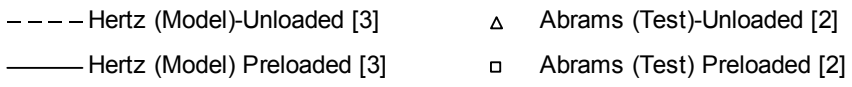

Fig. 3. Effect of preloading on concrete compressive strength at elevated temperature.

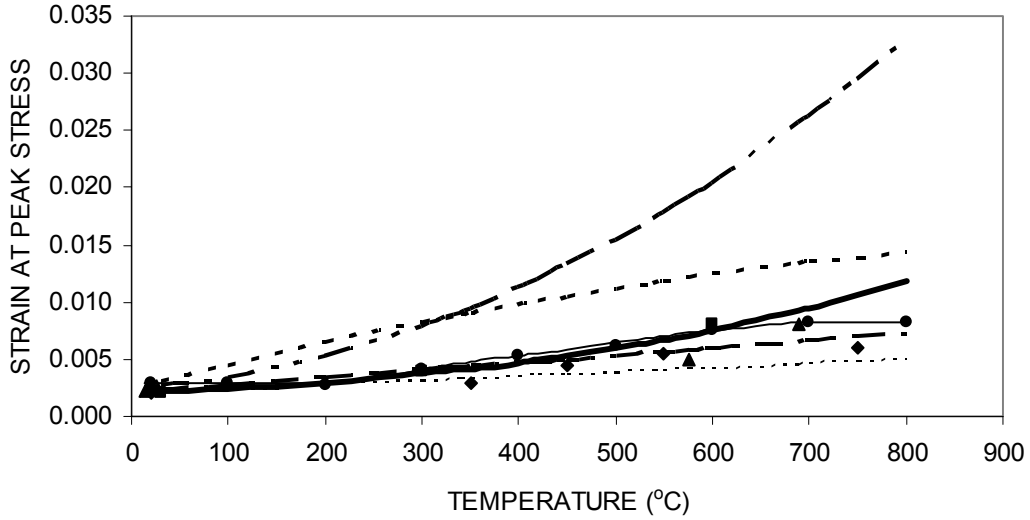

(a) Unstressed concrete.

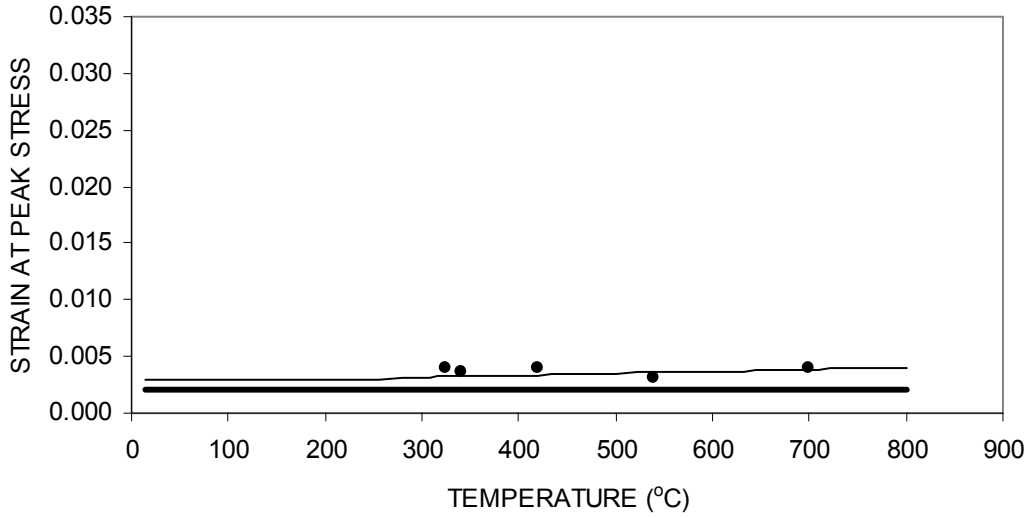

(b) Preloaded concrete.

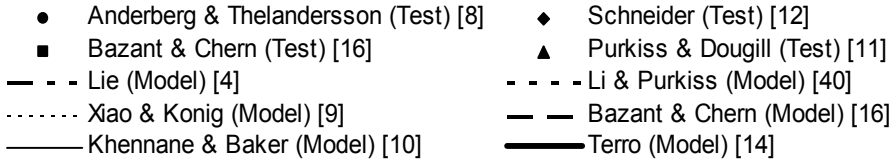

Fig. 4. Relationship between concrete strain at peak stress and temperature.

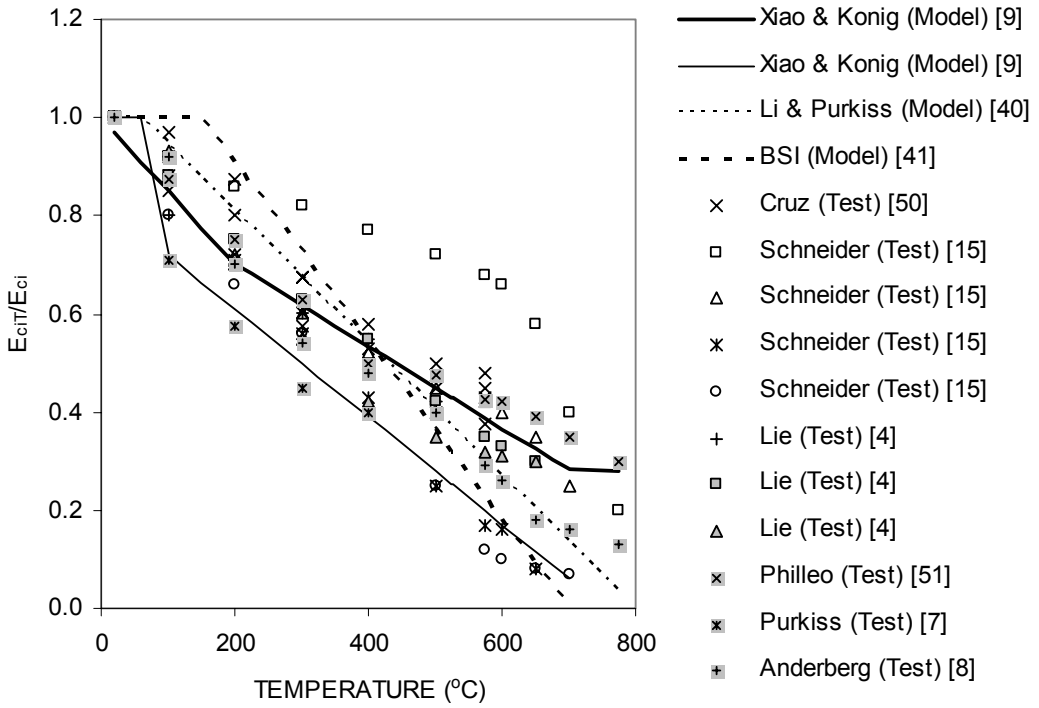

(a) Predictions of first group of analytical models.

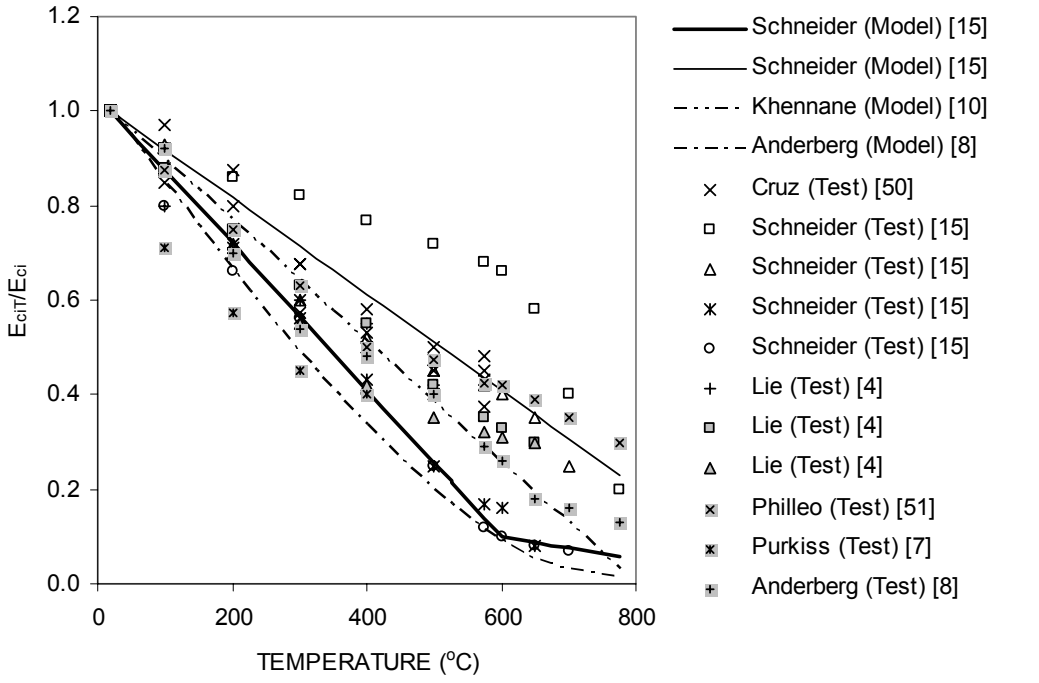

(b) Predictions of second group of analytical models.

Fig. 5. Initial Modulus of elasticity at elevated temperature (unstressed concrete).

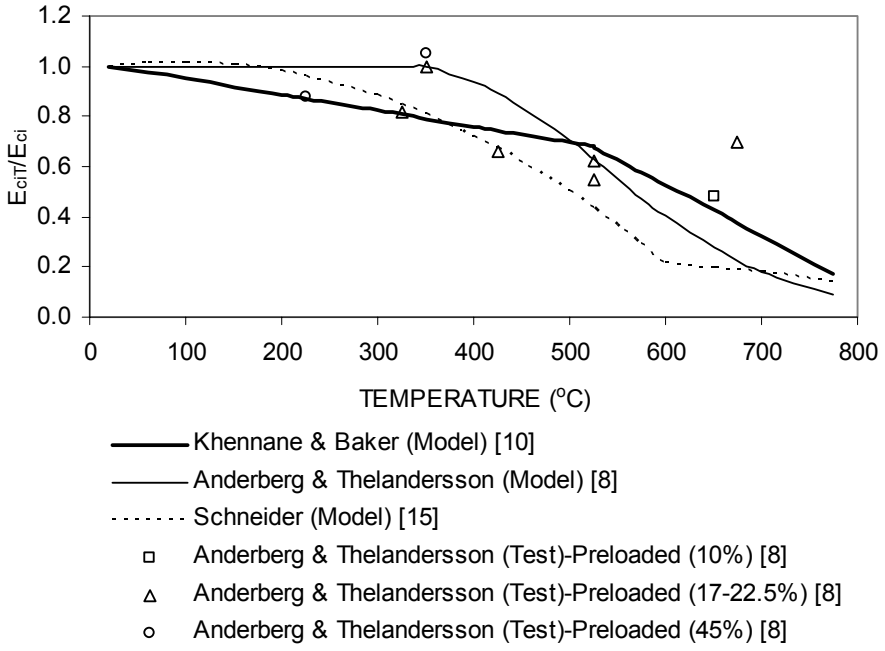

Fig. 6. Initial modulus of elasticity at elevated temperature (preloaded concrete).

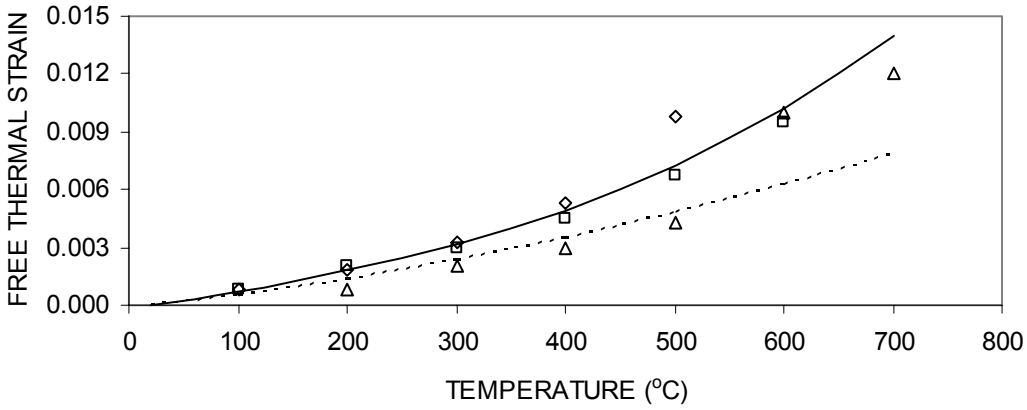

(a) Concrete with siliceous aggregates.

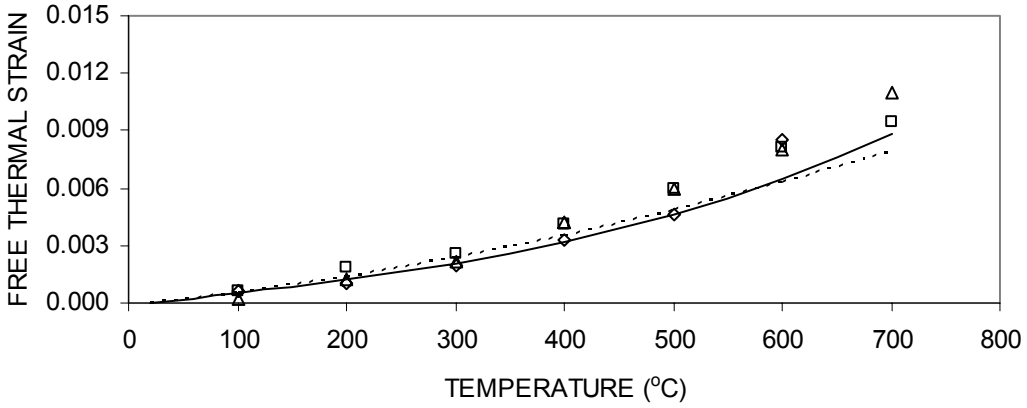

(b) Concrete with carbonate aggregates.

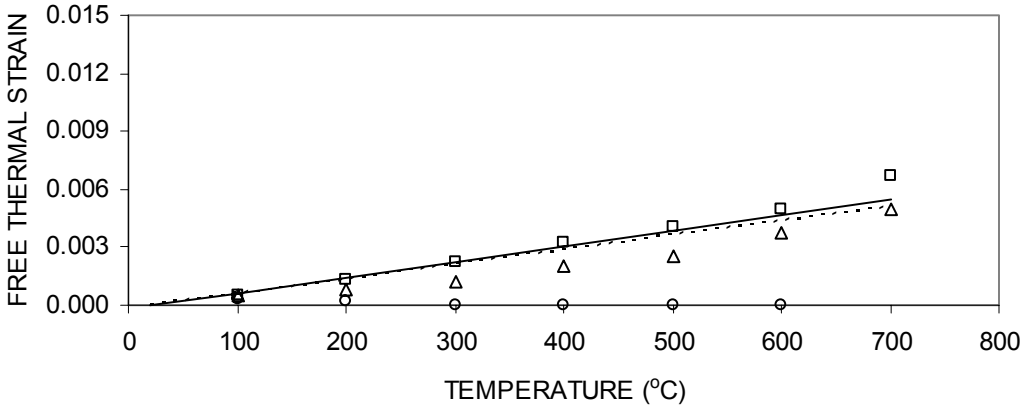

(c) Concrete with lightweight aggregates.

Fig. 7. Free thermal strain at elevated temperature.

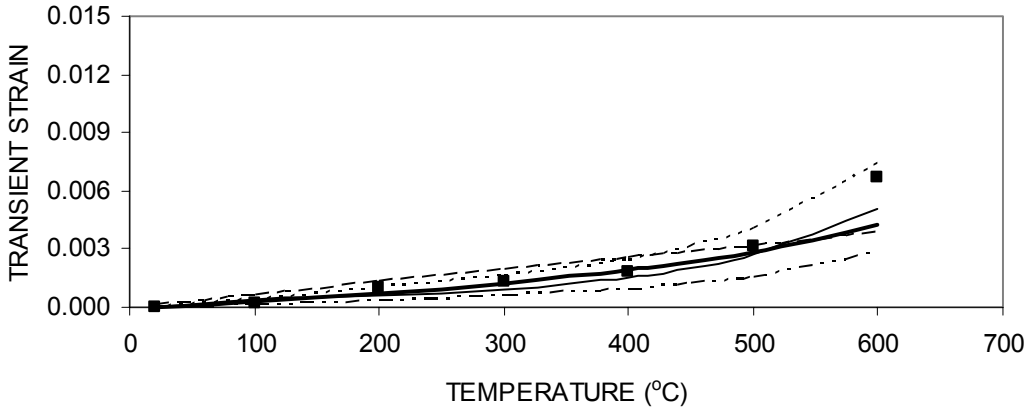

(a) preloading stress = $0.167\,f_c'$.

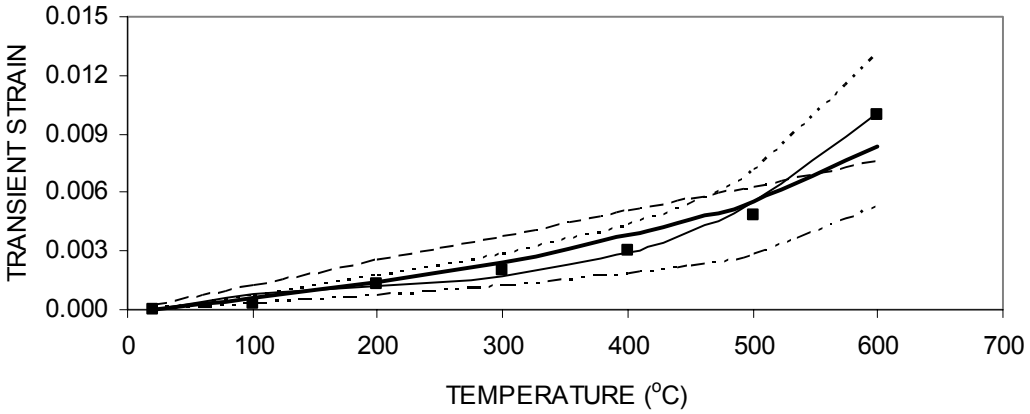

(b) preloading stress = $0.33\,f_c'$.

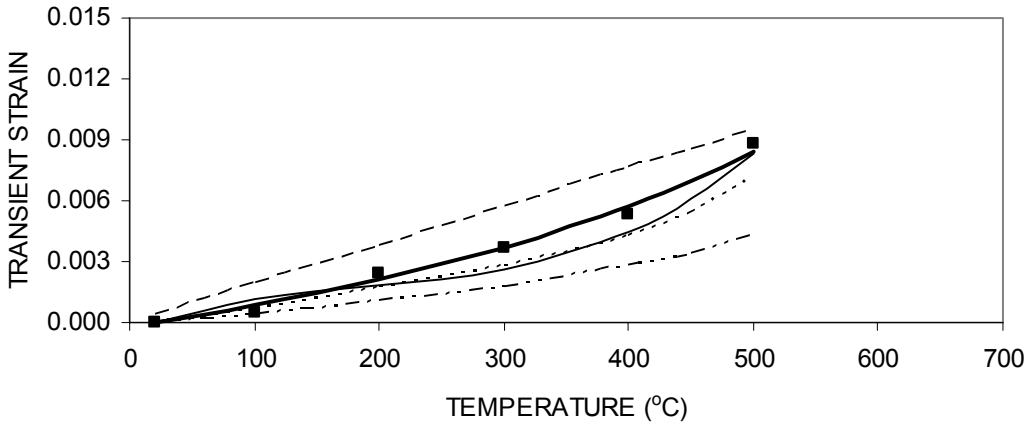

(c) preloading stress = $0.5\,f_c'$.

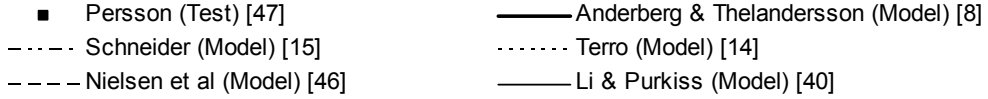

Fig. 8. Relationship between transient creep strain and temperature for different preloading stress levels.

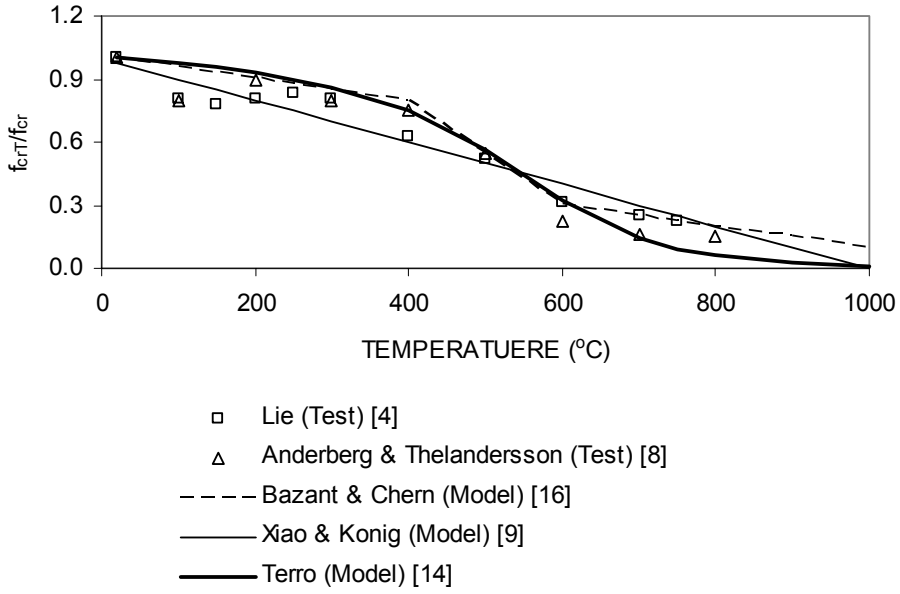

Fig. 9. Concrete tensile strength at elevated temperature.

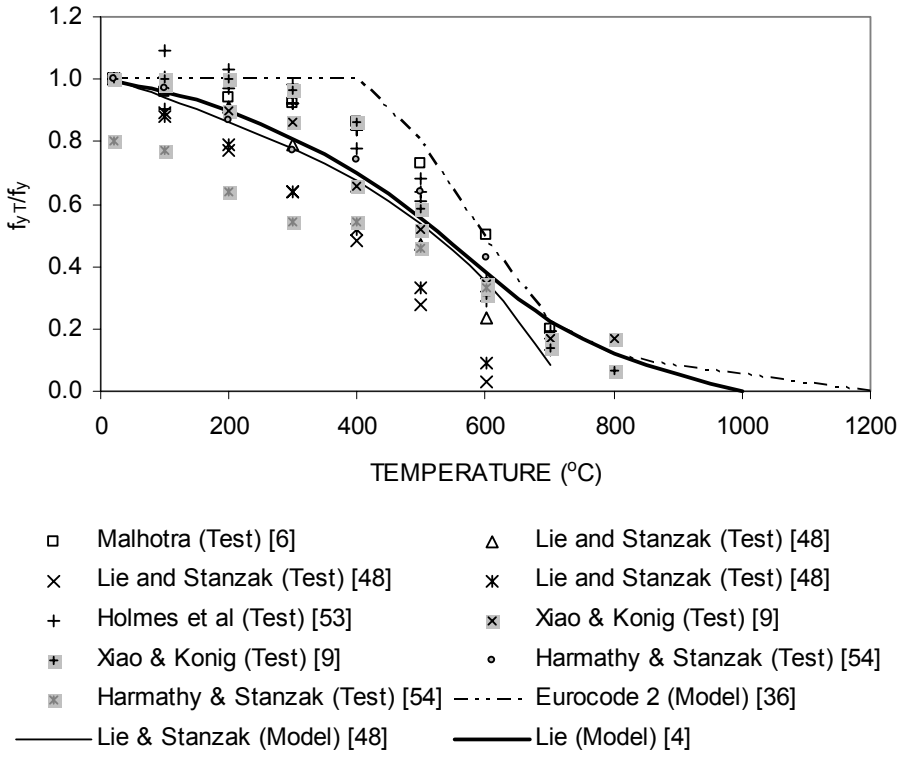

Fig.10. Steel yield strength at elevated temperature.

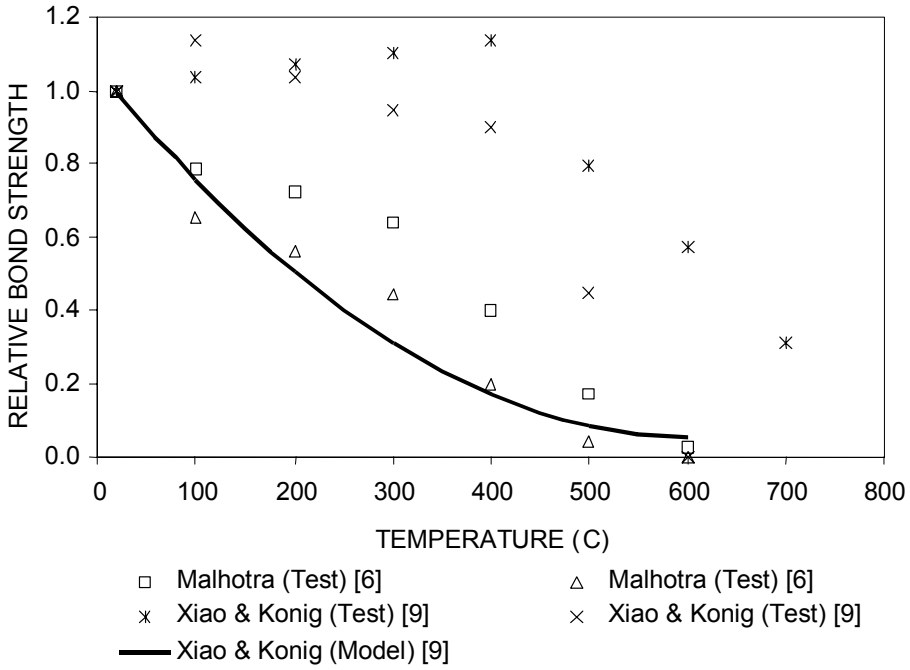

Fig. 11. Relative bond strength at elevated temperature.

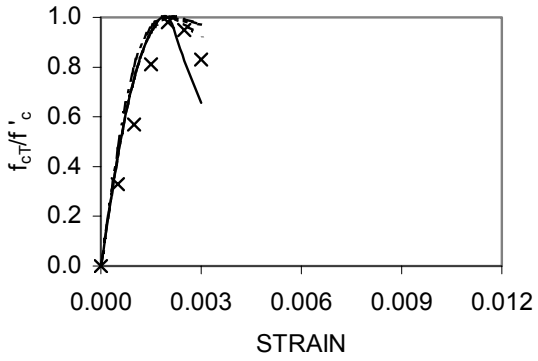

× Purkiss & Dougill (Test) [11]

(a) T= 15 °C

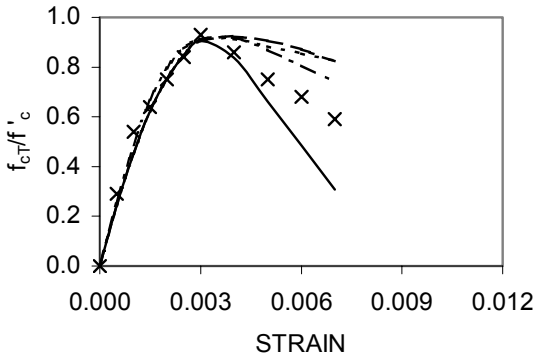

× Bazant & Chern (Test) [16]

(b) T= 300 °C

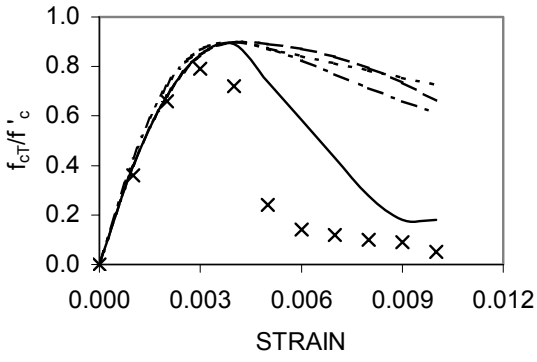

× Schneider (Test) [55]

(c) T= 350 °C

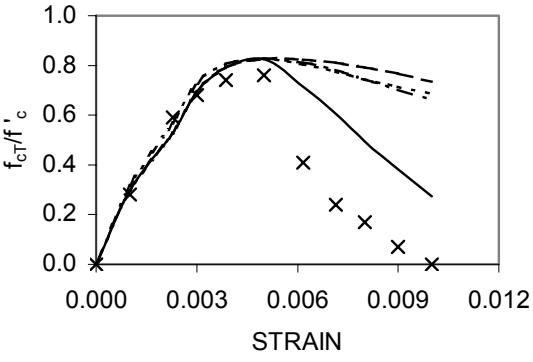

× Schneider (Test) [55]

(d) T= 450 °C

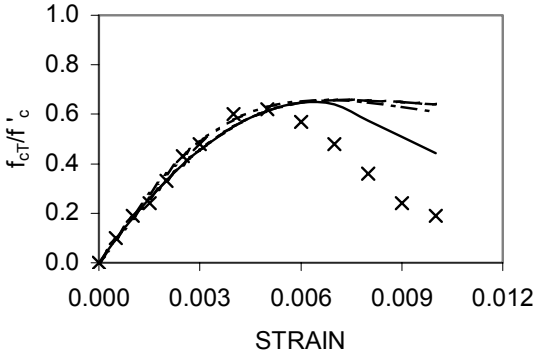

× Purkiss & Dougill (Test) [11]

(e) T= 575 °C

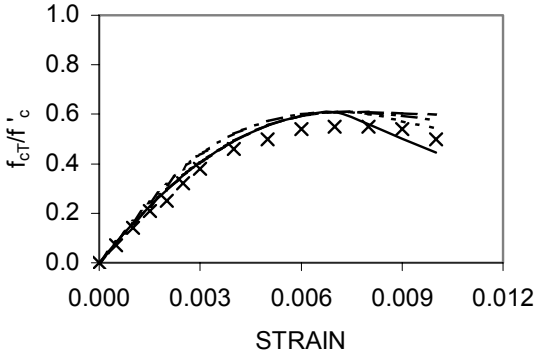

× Bazant & Chern (Test) [16]

(f) T= 600 °C

Anderberg and Thelandersson (Model) [8]
Analytical 1
Lie and Lin (Model) [38]
Analytical 2

Fig. 12. Instantaneous stress-strain curves at elevated temperature.

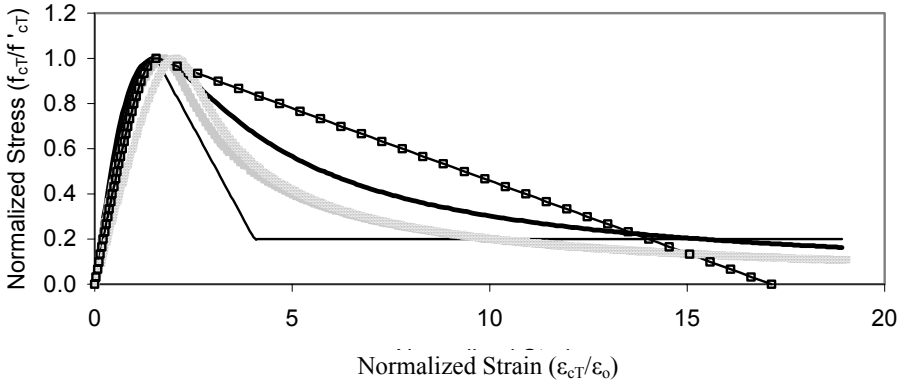

(a) T=100 °C

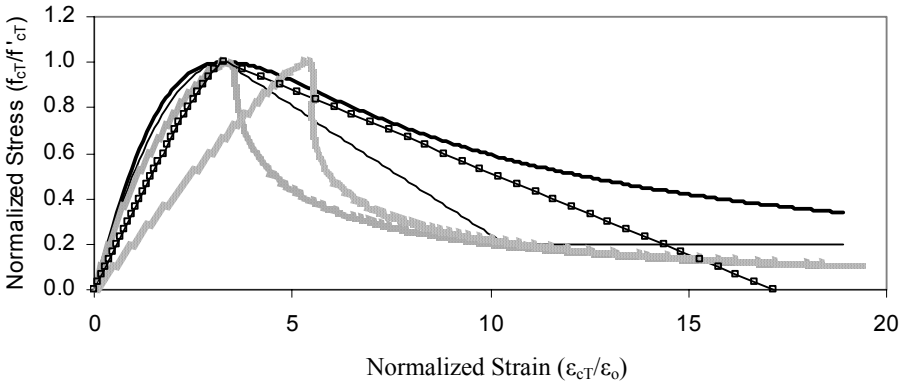

(b) T=300 °C

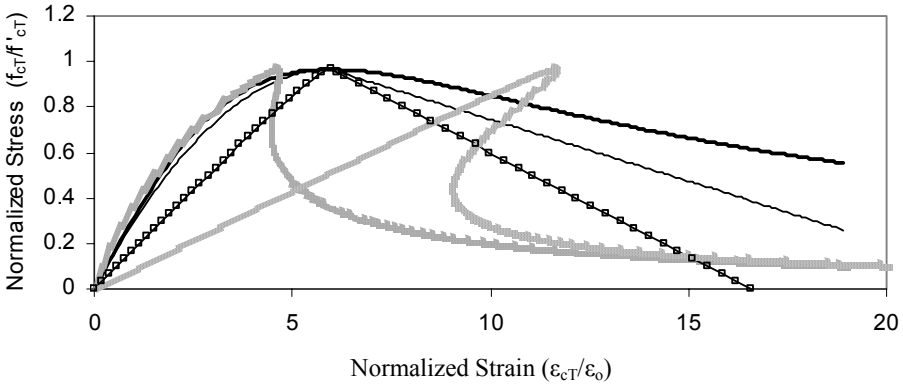

(c) T=500 °C

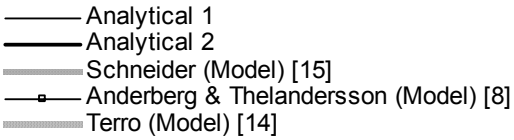

Fig. 13. Effect of transient creep on the stress-strain curve at elevated temperature.

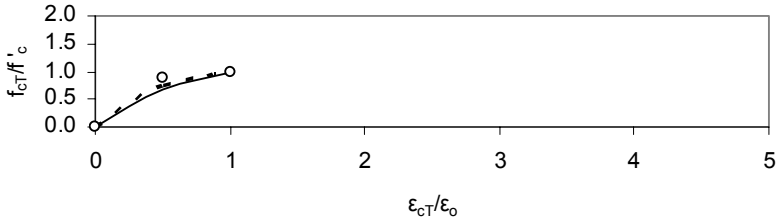

(a) T= 20°C

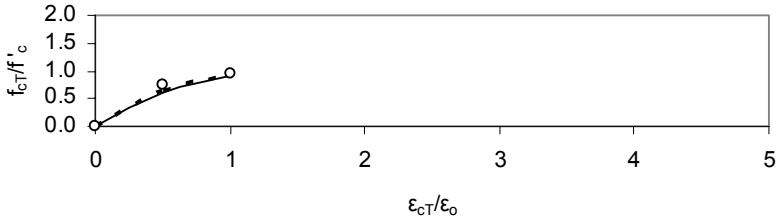

(b) T= 100°C

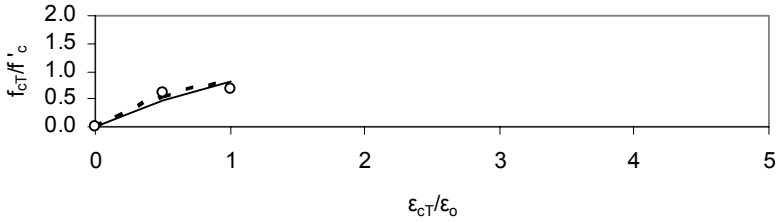

(c) T= 200°C

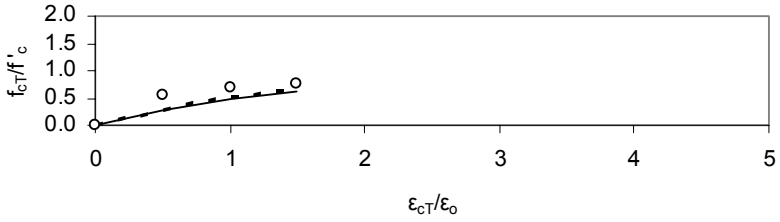

(d) T= 400°C

——— Analytical 1 - - - - Analytical 2 o Terro & Hamoush (Test) [56]

Fig. 14. Stress-strain curves for unconfined concrete cylinders.

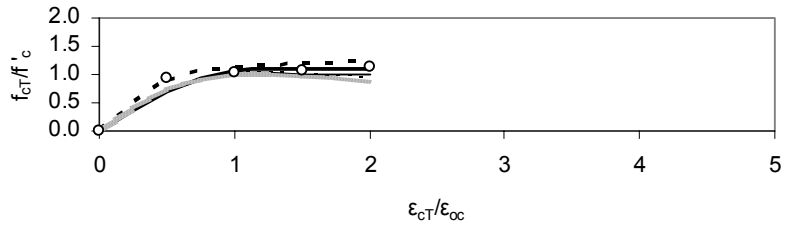

(a) T= 20°C

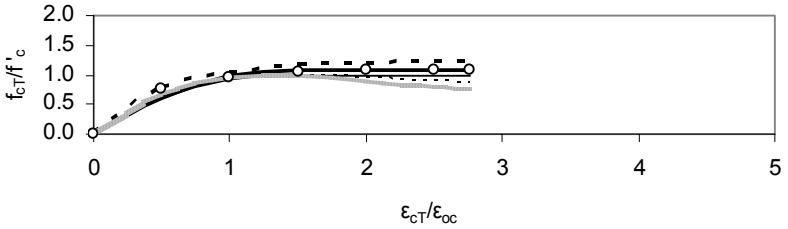

(b) T= 100°C

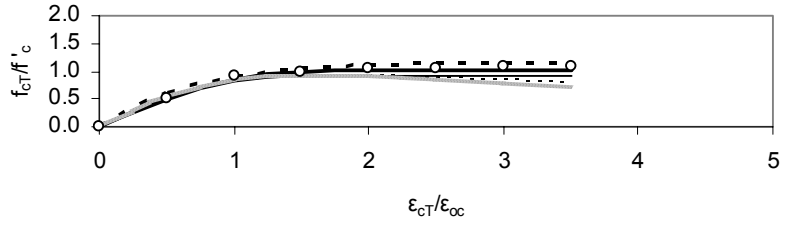

(c) T= 200°C

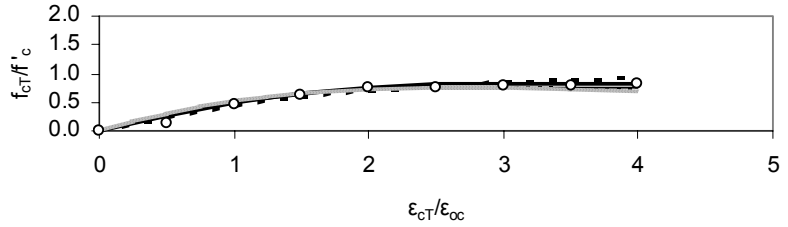

(d) T= 400°C

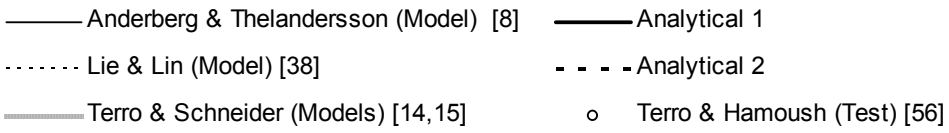

Fig. 15. Stress-strain curves for concrete cylinders confined by 6 circular stirrups.

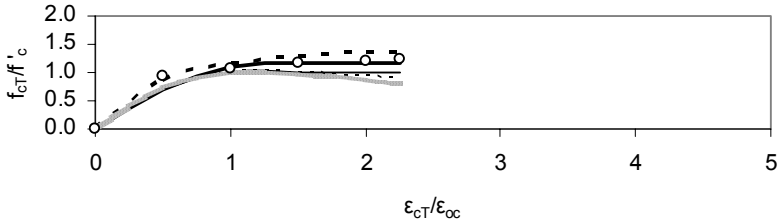

(a) T= 20°C.

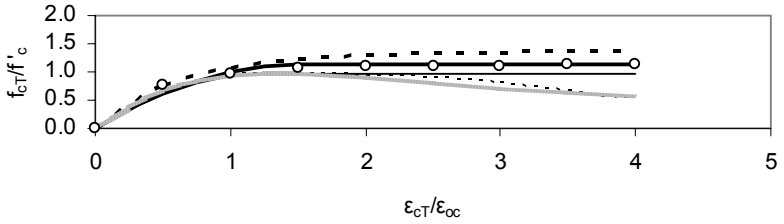

(b) T= 100°C.

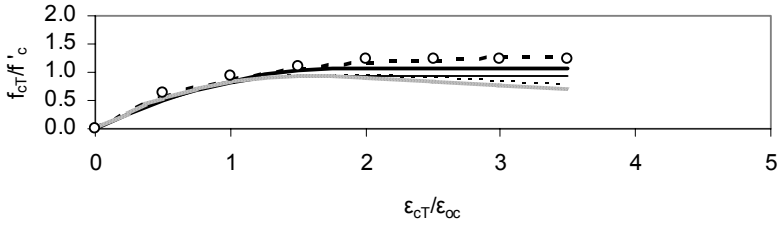

(c) T= 200°C.

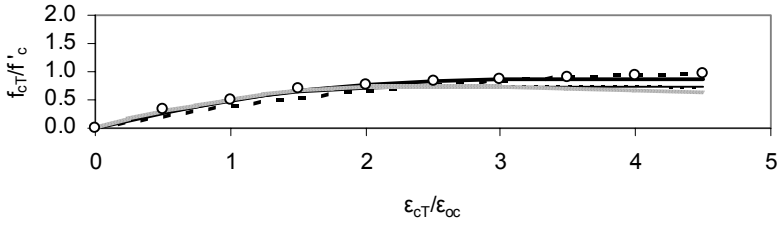

(d) T= 400°C.

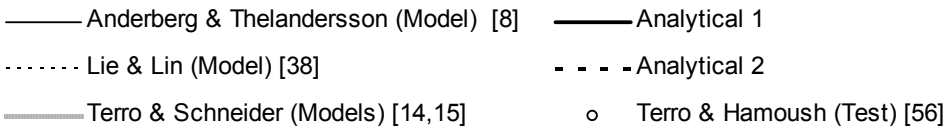

Fig. 16. Stress-strain curves for concrete cylinders confined by 9 circular stirrups.